NASA TN D-1057

TECHNICAL NOTE

D-1057

ANALYSIS OF X-15 LANDING APPROACH AND FLARE CHARACTERISTICS DETERMINED FROM THE FIRST 30 FLIGHTS

By Gene J. Matranga

Flight Research Center
Edwards, Calif.

NATIONAL AERONAUTICS AND SPACE ADMINISTRATION

WASHINGTON

July 1961

1J

NATIONAL AERONAUTICS AND SPACE ADMINISTRATION

TECHNICAL NOTE D-1057

ANALYSIS OF X-15 LANDING APPROACH AND FLARE CHARACTERISTICS DETERMINED FROM THE FIRST 30 FLIGHTS

H
2
2
1

By Gene J. Matranga

SUMMARY

The approach and flare maneuvers for the first 30 flights of the X-15 airplane and the various control problems encountered are discussed. The results afford a relatively good cross section of landing conditions that might be experienced with future glide vehicles having low lift-drag ratios.

Flight-derived drag data show that preflight predictions based on wind-tunnel tests were, in general, somewhat higher than the values measured in flight. Depending on configuration, the peak lift-drag ratios from flight varied from 3.5 to 4.5 as compared with a predicted range of from 3.0 to 4.2.

By employing overhead, spiral-type patterns beginning at altitudes as high as 40,000 feet, the pilots were consistently able to touch down within about ±1,000 feet of a designated point.

A typical flare was initiated at a "comfortable" altitude of about 800 feet and an indicated airspeed of approximately 300 knots, which allowed a margin of excess speed. The flap and gear were extended when the flare was essentially completed, and an average touchdown was accomplished at a speed of about 185 knots indicated airspeed, an angle of attack of about 7°, and a rate of descent of about 4 feet per second.

In general, the approach and landing characteristics were predicted with good accuracy in extensive preflight simulations. F-104 airplanes which simulated the X-15 landing characteristics were particularly valuable for pilot training.

INTRODUCTION

Prior to the first flight of the X-15, it was apparent from wind-tunnel tests that the landing approach and flare maneuvers would be performed in a range of lift-drag ratios lower than previously flown with rocket-propelled aircraft (ref. 1). Since piloting problems were anticipated, analytical and flight-test studies were undertaken by the NASA Flight Research Center, the manufacturer (North American Aviation, Inc.), and the Air Force Flight Test Center to determine how well the pilot could execute approach and flare maneuvers at reduced lift-drag ratios. References 1 to 3 are illustrative of these investigations.

This paper expands upon the limited analyses of early X-15 landings presented in references 1, 4, and 5. The landing approach and flare data acquired during the first 30 X-15 flights are considered in detail and are compared with the preflight predictions. Included are data for the initial landings of each of the seven X-15 pilots. These results, it is believed, are generally indicative of flight characteristics and piloting problems which might be encountered in executing a normal flared landing with future low-lift-drag-ratio gliders.

A detailed analysis of the X-15 landing-gear behavior during touchdown and runout is presented in reference 6.

SYMBOLS

a_n	normal acceleration, g units
C_D	airplane drag coefficient
C_L	airplane lift coefficient
g	acceleration due to gravity, ft/sec^2
h	geometric altitude (referenced to touchdown point), ft
L/D	lift-drag ratio, C_L/C_D
M	Mach number
p	rolling velocity, deg/sec
q	pitching velocity, deg/sec
t	time before touchdown, sec

Δt incremental time before touchdown, sec

V_i indicated airspeed, knots

V_v vertical velocity, ft/sec

W landing weight, lb

x longitudinal distance from touchdown, ft

Δx touchdown dispersion from intended touchdown point, ft

y lateral distance from touchdown, ft

α angle of attack, deg

β angle of sideslip, deg

δ_a aileron deflection (left horizontal-tail deflection minus right horizontal-tail deflection), deg

δ_f flap deflection, deg

δ_h horizontal-tail deflection, $\frac{\text{Left horizontal-tail deflection + Right horizontal-tail deflection}}{2}$, deg

Subscripts:

The following subscripts apply to conditions during the particular portion of the landing approach and flare maneuver indicated.

f flare initiation

g_e gear extension

TD touchdown

90 pattern base leg

180 pattern downwind leg

f_e flap extension

max maximum condition during flare

AIRPLANE

The X-15 is a single-place research airplane designed to perform at speeds up to 6,600 ft/sec and altitudes up to 250,000 feet. The peak performance is attained during short-duration, rocket-powered flight following which the airplane performs an unpowered glide to the landing. A three-view drawing of the airplane is shown in figure 1. Figure 2(a) is a photograph of the airplane in the normal ground attitude, and figure 2(b) shows the airplane in flight just prior to main-gear touchdown. Table I contains pertinent X-15 physical characteristics.

The airplane has a 5-percent-thick wing with an aspect ratio of 2.5. Plain flaps are located at the trailing edge of the wing.

All aerodynamic control surfaces are actuated by irreversible hydraulic systems. Movable horizontal-tail surfaces are deflected essentially symmetrically for longitudinal control and differentially for lateral control by means of either a conventional center stick or a side-located controller. The controllers are linked mechanically and hydraulically to provide simultaneous movement of both control sticks; however, to obtain a given stabilizer motion, only about one-third as much movement of the side stick is required as of the center stick. The movable portions of the upper and lower wedge-sectioned vertical tails, actuated by conventional rudder pedals, provide directional control. Just prior to flare initiation, the lower movable portion of the vertical tail (also referred to as the movable rudder) is jettisoned to allow sufficient ground clearance for landing. Speed brakes are located on the rear fixed portion of the upper and lower vertical tails.

Augmented aerodynamic damping of the airplane is provided about all three axes in a conventional manner. An additional interconnect damper, termed "yar", furnishes a crossfeed of the yaw-rate signal into the roll damper. The characteristics of the stability augmentation system are given in table II.

A nominal flap deflection of 40° was used for the first five flights of the number 1 X-15 airplane and the first three flights of the number 2 airplane. However, in order that a reduced drag could be obtained without appreciably affecting the lift, the nominal deflection was reduced to 30° for all subsequent flights. The actual flap deflection recorded during each flight and the flap-actuation time are included in the tabulation of flight-measured characteristics in table III.

The landing gear consists of a comparatively conventional dual-wheel nose gear located far forward of the airplane center of gravity and steel skids located to the rear under the horizontal tail (fig. 1).

Extensive detail of this gear system and its operation is presented in reference 6. Table III lists the gear-actuation time for each flight.

INSTRUMENTATION

The following quantities pertinent to this investigation were recorded on NASA internal-recording instruments, synchronized by a common timer:

Airspeed and altitude
Normal and longitudinal acceleration
Angle of attack and angle of sideslip
Rolling, yawing, and pitching velocity
Aileron, vertical-tail, horizontal-tail, and flap deflection

The airspeed and pressure altitude were measured with a conventional NASA pitot-static tube mounted on a nose boom. A description of the nose boom and its accuracies is given in reference 7. Also on the nose boom were free-floating vanes used to measure angles of attack and sideslip. The angles presented in this paper were not corrected for transient position errors, since these errors were considered negligible. The angular velocities were measured about the airplane body axes.

Geometric altitude and ground coordinates for the approach-pattern analysis were obtained from multistation solutions of position data furnished by Air Force Flight Test Center Askania cinetheodolite cameras. These cameras, operating at 4 frames per second, tracked the airplane throughout the pattern, flare, touchdown, and ground runout. Akeley phototheodolite cameras, running at 19 frames per second, tracked the airplane through the final phases of the flare, the touchdown, and ground runout. A combination of the Askania and Akeley camera data provided altitude and rate-of-descent information during the flare and touchdown.

During some of the more recent landings reported in this paper, an analysis of the skid imprint on the lakebed (see ref. 6) and measurements using the skid itself as a trailing arm (somewhat similar in principal to the method of ref. 8) afforded additional cross checks for determining the value of rate of sink at touchdown. The values obtained from these independent sources generally agreed to within 1 ft/sec.

TEST CONDITIONS

Table III presents a listing of the pilot, landing weight, damper setting, and control stick used during the flare, together with conditions existing on the downwind and base legs of the pattern, at flare initiation, during flap and gear extension, and at touchdown for each flight. This tabulation forms the nucleus of this paper and will be referred to frequently in the subsequent sections. In the flight designation used in the first column of the table, the first digit indicates the airplane by number (1 or 2), the second indicates the free-flight number of the particular airplane, and the third indicates the total airborne X-15/B-52 flights for that airplane.

At least one landing has been performed by each of the seven X-15 pilots (A to G in the tabulation). Three were NASA pilots, two were Air Force pilots, one was a U.S. Navy pilot, and one was a North American Aviation pilot.

Weights at touchdown have ranged from a low of 13,234 pounds which was experienced on the initial glide flight (1-1-5), as discussed in reference 4, to a high of 15,183 pounds recorded on flight 2-3-9. The average touchdown weight was about 14,600 pounds, which corresponds to a wing loading of 73 lb/sq ft.

The numbers in the column labeled damper setting indicate the settings for the pitch, roll (plus yar), and yaw dampers, respectively, for each flight. The relationship between damper setting and gain is presented in table II. Damper gains have varied from all dampers off for flight 2-8-16 to all dampers on at the setting of 4-4-8 used for most of the flights. The landing of flight 2-8-16 was made intentionally with all dampers off. In flights 1-1-5, 2-2-6, 2-3-9, 1-2-7, 1-3-8, and 1-6-11, the zero gain for one damping mode was caused by a malfunction in that particular mode.

The side stick was utilized to perform the flare on only the initial flight (1-1-5) and two subsequent flights (2-9-18 and 2-10-21). On all other flights the conventional center stick was used.

Pattern geometry varied from S-shaped patterns to full 360° overhead patterns, depending on space-positioning requirements at the high key or initial point.

All landings reported herein were made on designated runways on the hard surface of Rogers Dry Lake at Edwards Air Force Base, Calif., except for flight 2-3-9. This flight terminated in an emergency landing on nearby Rosamond Dry Lake following an in-flight explosion in the engine compartment. Figure 3 is an aerial photo map of

Rogers Dry Lake, showing the marked lakebed runways. The initial landing and 10 subsequent landings were performed on the longest Rogers Dry Lake runway, designated as 1 in figure 3. Seventeen landings were performed on the runway designated as 2. Also, because of appreciable cross winds on runway 1, the pilot for flight 1-5-10 elected to land on the runway labeled 3.

For the first five flights of the number 1 airplane and the first three flights of the number 2 airplane, the nominal flap deflection for touchdown was 40°. Subsequent flights were performed with a nominal 30°-flap deflection at touchdown.

RESULTS AND DISCUSSION

To provide general information on the ranges of lift, drag, and angle of attack covered in this study, the following section presents, first, performance data for the X-15 in various landing configurations. This is followed by a discussion of the approach patterns flown and the flare maneuvers performed prior to landing. These maneuvers are graphically illustrated by typical time histories and summary plots. Finally, an assessment is made of the extensive in-flight simulations employed in the flight program, with particular attention to the value of such simulations and their applicability to future low-lift-drag-ratio gliders.

Performance

Figure 4 presents angle of attack, lift-drag ratio, and drag coefficient as a function of lift coefficient for the X-15 in various approach configurations. All data were measured during approach and flare maneuvers and are thus representative of the lift and angle-of-attack range covered during this portion of the landing. Because of the transient nature of the flare and the relatively short intervals during which the airplane remained in some fixed configurations (notably, those with the flaps extended only) data in several configurations are limited. Also shown in this figure are the manufacturer's estimates of these variables based on wind-tunnel data.

Clean airplane.- Figure 4(a) presents the performance data for the clean airplane at approach speeds ($M \approx 0.5$ to 0.7). The flight-measured peak lift-drag ratio is about 4.25, occurring at a lift coefficient of about 0.45 and an angle of attack of approximately 8°. With few exceptions, the pilots have flown on the "front side" (low C_L) of the L/D curve throughout the approach pattern. The low-lift condition is maintained by increasing bank angle as normal acceleration is increased

at constant speed or by increasing bank angle or decreasing normal acceleration, or both, as speed is reduced. This trend is normal, since pilots usually like to allow some margin for reducing glide angle by increasing lift. The estimates of the lift curve agree well with the flight data, although a slight discrepancy between the flight and predicted drag due to lift is evident. Fortunately, the predicted lift-drag ratios were somewhat lower than those measured in flight; therefore, the actual landing problem was somewhat less than anticipated. Similar trends were evident in the data of reference 9 at higher subsonic Mach numbers.

Ventral off.- Prior to flare initiation, at an altitude of several thousand feet, the lower X-15 rudder is jettisoned. Data for this configuration are presented in figure 4(b). Jettisoning the ventral increases the peak lift-drag ratio to about 4.5 and slightly decreases the lift coefficient for the peak lift-drag ratio. Again there are few data points on the "back side" of the L/D curve and, as before, minor differences exist between the flight and predicted data.

Flaps extended.- As noted previously, only eight landings were performed with a nominal flap deflection of 40° (lower rudder off), and, since this configuration existed only briefly in these flights, data in this configuration are limited, as shown in figure 4(c). Although the data seem to agree reasonably well with predictions, they are insufficient to define any trends.

Data obtained with the ventral off and a 30°-flap deflection are presented in figure 4(d). All data are on the front side of the L/D curve, with no definite peak discernible. In this instance, both the predicted drag due to lift and the lift-curve slopes differ from values obtained in flight.

Landing configuration.- Representative data in the landing configuration (ventral off, flap and gear extended) with a flap deflection of 40° are presented in figure 4(e). The peak lift-drag ratio of 3.3 occurs at a lift coefficient of about 0.55 and an angle of attack of about 7°. In this instance, the lift-drag-ratio data are distributed on both sides of the peak and are noticeably higher than predicted, especially at low lift. It should be noted that the flight data in this figure do not concur with those previously reported in reference 4. The latter data were obtained under transient conditions with comparatively insensitive accelerometers and, therefore, are considered to be less accurate than the data of figure 4(e).

Figure 4(f) presents data for the landing configuration with lower rudder off, flaps deflected 30°, and gear extended. The peak lift-drag ratio is about 3.5 and occurs at a lift coefficient of about 0.6 and an angle of attack of about 7°. Most of the data are on the front side of

the L/D curve; however, some data do exist on the back side. The flight-measured values for lift-curve slope and lift-drag ratio are again higher than predicted.

Summary.- Faired values of the flight-measured lift-drag ratios are plotted against lift coefficient in figure 5 for the various X-15 configurations. For the configurations where the flaps are extended, only curves for 30°-flap deflection are shown inasmuch as this condition is most indicative of that which is currently being utilized on the airplane. The peak lift-drag ratio of 4.25 in the clean configuration can be raised to 4.5 by jettisoning the ventral, thereby offering a potential means of increasing range capability. Deflecting the flaps 30° causes no appreciable change in the peak lift-drag ratio. As expected, however, there is a reduction in the trim angle of attack through the period of flap extension. In the landing configuration (ventral off, $\delta_f = 30°$, gear extended), the peak lift-drag ratio is 3.5. The data on the back side of the L/D curves result primarily from landings performed at a speed lower than that for peak lift-drag ratio, rather than from large normal accelerations during the flare. Before touchdown is accomplished, speed can be inadvertently reduced below that for peak lift-drag ratio ($C_L > 0.6$), since the speed decay with the flaps and gear extended is of the order of 6 KIAS per second.

Pattern

Several representative X-15 approach patterns are shown in figure 6 for approach speeds averaging about 300 knots indicated airspeed. An S-pattern and 270° and 360° overhead patterns are illustrated. For the 360° overhead pattern, the high key point is greater than 20,000 feet above the touchdown point. (In this paper, high key is defined to be the point where the pilot terminates his glide to the landing site and initiates his spiral turn to the touchdown point.) For the patterns shown, the average altitude is about 12,000 feet on the downwind leg and about 6,000 feet on the base leg. The average radius of turn in these patterns is of the order of 10,000 feet.

As mentioned in reference 4, digitally computed preflight predictions of pattern geometry were good. Figure 7 shows a comparison of flight and predicted patterns. The flight pattern is somewhat tighter than the predicted path, even though the flight-determined lift-drag ratio was higher than predicted (as seen in fig. 4). This reflects the slightly higher speed and bank angle preferred by the pilot in flight as compared with predictions.

Pattern selection.- By referring to table III, the type of pattern flown and the speed, altitude, and space-position coordinates on the downwind leg and base leg of the patterns can be compared from flight to

flight. From this tabulation it can be seen that there is no predominance of any particular type of pattern, except that all patterns utilized at least 180° of turning flight. The pattern selected depended primarily on space-positioning considerations at the high key point. The S-pattern and the 180° pattern were utilized most frequently on initial flights because they were the most convenient for the type of ground tracks traversed on these flights (see refs. 4 and 5).

Downwind leg.- Conditions at the maximum lateral distance from the touchdown point were chosen as representative for the downwind leg of each flight in table III. On 180° patterns where there was no point of inflection, the point directly opposite the touchdown point ($x_{180} = 0$) was selected as the downwind coordinate.

Speeds on the downwind leg varied from as low as 247 KIAS to as high as 332 KIAS. The lowest altitude was 7,782 feet, whereas the highest was 25,293 feet. Lateral separations from the touchdown on the downwind leg ranged from 13,557 feet to 34,244 feet.

Base leg.- For the base leg of the pattern, conditions at the maximum longitudinal distance from the touchdown point were chosen as representative.

Speeds on the base leg of the pattern, as shown in table III, ranged between 246 KIAS and 338 KIAS. Altitudes varied between 3,479 feet and 12,394 feet, and longitudinal distance from the touchdown varied between 13,878 feet and 34,386 feet.

Summary.- Figure 8 shows the spread of the patterns flown during the first 30 landings of the X-15. The ranges of the pattern space-position data are indicated as shaded areas. The pattern of flight 1-13-25 is considered an exception to the data presented herein and, thus, is shown individually. On this flight an engine failure at the most distant point in the flight trajectory was encountered and the pilot, concerned about returning to the base successfully, performed the pattern shown. This landing emphasizes the wide range of landing flexibility of even this low-lift-drag-ratio vehicle and the adaptability of the pilot.

In general, the pilots encountered no serious problems in performing the approach maneuver. The airplane had satisfactory control effectiveness at approach speeds, and the visibility in the landing maneuver was adequate for a research-type airplane. All pilots performed circling patterns which were generally flown with some excess in speed ($V_i \approx 300$ KIAS) to compensate for uncertain wind conditions and possible misjudgment of distances. The excess energy was then expended through use of speed brakes and maneuvering flight prior to entry into the final approach. The resulting convergence of the

patterns is readily evident in figure 8 which, in turn, emphasizes the great amount of flexibility that is available in a circling pattern (ref. 1).

Rates of descent in the pattern have been as high as 400 ft/sec at high speeds with the speed brakes extended. However, the average rate of sink is nearer 275 ft/sec. This value is considerably greater than the limiting rate of sink recommended in reference 10. Because of the consistent use of high sink rates in the X-15 landing patterns as well as in other tests (refs. 1 to 3, 11, and 12), the specification of a limiting rate of descent applicable to all vehicles is not believed to be realistic. The choice of a limiting rate, instead, should be based on a number of factors, such as normal approach and flare speeds, glide angles, vehicle lift capability, available time before touchdown, and the repeatability of the landing from a piloting standpoint.

Flare

Since most problems involved in landing the X-15 occurred during the first few landing flares, each of the first four flights is discussed in detail. Subsequent sections cover the effects of technique, dampers, side-stick controller, and flap extension on the flare and the relationship of these variables to problems encountered in the initial flights. Finally, a summary of flare parameters is presented and discussed. First, however, the results of a preflight study of configuration effects are considered.

Preflight configuration study.- Well in advance of the first X-15 flight, both flight and analog simulation studies were conducted to define the optimum flare technique to use. From this study it was determined that flap and gear extension should be delayed until the flare was essentially completed. The comparison of two analog time histories in figure 9 shows the advantage of this procedure. In one maneuver, the flaps and gear are extended at the beginning; in the other, the flaps and gear are extended near the end of the flare. The flare-initiation speed was 300 KIAS for both maneuvers. In the first maneuver, however, the flare was initiated at an altitude of about 2,000 feet and a rate of sink of slightly less than 290 ft/sec; for the second maneuver, the altitude was only 800 feet and the rate of sink about one-half that of the preceding maneuver. The flaps and gear were then extended at 350 feet. It is obvious, as discussed in reference 2, that the latter technique would afford the pilot the time and margin for error in determining the flare-initiation point that is consistent with normal pilot capability and judgment.

First flight (1-1-5).- Details of this glide flight were reported in reference 4. Since it was an intentional unpowered flight and no

propellants were carried, the landing weight of 13,234 pounds is the lowest recorded to date. Prior to pattern entry, the pilot performed a stall approach in the clean configuration and extended the flaps for an evaluation. The flaps were then retracted, and the landing pattern was entered. During these maneuvers, the lack of a pitch damper (which had failed before launch) posed no problems. Because of time limitations, the pilot was able to perform only these limited maneuvers in evaluating the handling qualities that might be expected in the approach and flare. Throughout the entire flight, the pilot controlled the airplane with the side-located controller.

Figure 10 is a time history of the events which occurred on this flight during the flare. At an altitude of 1,591 feet and an airspeed of 270 KIAS the pilot initiated the flare. About 8 seconds later the flaps started down. Near the end of the flap cycle, severe longitudinal oscillations developed, with peak-to-peak oscillations in angle of attack reaching values as high as ±5°. In attempting to subdue this motion, the pilot repeatedly attained the limit angular rate of the horizontal stabilizer (15 deg/sec), as indicated by the saw-tooth motion in figure 10. Touchdown was finally accomplished at an airspeed of 153 KIAS with a rate of descent of 2 ft/sec and, fortunately, because of restrictions on angle of attack, at the bottom of an oscillation where the angle of attack was only 8.5°.

Immediate analysis of the flight records (ref. 4) considered a number of possible contributing factors. These included the lack of automatic pitch damping, the existence of a nonlinear airplane pitching moment with near-neutral stability at low angle of attack, and an oversensitivity of the side-located control stick. Pilot impressions of this landing (see ref. 13, for example) indicate that, at the time, he believed the airplane to be statically unstable in the longitudinal mode. Subsequent six-degree-of-freedom analog simulations showed that the oscillations could only have been pilot-induced.

As a result of all these factors, it was decided by the manufacturer that (1) the less-sensitive center stick would be used in subsequent landings, (2) the control-surface rate would be increased from 15 deg/sec to 25 deg/sec, (3) the longitudinal-force gradient would be increased approximately 30 percent, (4) the longitudinal breakout force would be increased slightly, and, as an additional precaution, (5) launches would be performed only if the pitch damper were operating. These modifications were incorporated into the number 2 airplane. It was considered essential that these restrictions remain in effect until additional tests could be performed to justify relaxing the restrictions or further altering the control system. However, from additional tests, the NASA and the USAF determined that the higher force gradient and higher breakout force were not particularly desirable from a piloting standpoint. These changes were,

therefore, not incorporated into the number 1 airplane which was to be flown in the initial joint NASA, USAF, and Navy program. The surface rate was increased, though, and the restriction was observed of launching only if the pitch damper was operating.

Second flight (2-1-3).- An account of this first powered X-15 flight is given in reference 5. The flare time history for this flight (fig. 11) shows that the flare was initiated at an altitude slightly greater than 500 feet and at an airspeed of 242 KIAS. Shortly thereafter, the flap cycle was started. Although at first, as can be seen in the figure, the flap motion proceeded at a normal rate, the rate of extension after only 2 seconds of operation decreased abruptly. Consequently, at touchdown only about 60 percent of the total flap travel had been reached. With the pitch damper operating normally and the center stick being used for control, the only transient noticeable to the pilot occurred with gear extension. This, however, was quickly damped. Touchdown was accomplished at an airspeed of 184 KIAS, a rate of sink of 4 ft/sec, and an angle of attack of 8.1°.

Although the flap failed to operate properly and the pilot prolonged the flare to the point of touchdown (indicated on the vertical-velocity trace of fig. 11), this landing was comparatively successful. Some of the concern generated by the first landing was, therefore, dispelled.

Third flight (2-2-6).- On this flight the roll damper failed at launch. However, as anticipated from preflight simulator tests, this created no serious control problem. Figure 12 presents a time history of the flare. With the pitch damper operating and the pilot using the center stick, the flare was executed from an altitude of 700 feet at an airspeed of 244 KIAS. The flap extended properly and did not introduce any serious transients. Because of the lack of an energy margin, the pilot was again forced to extend the flare to the point of touchdown, which resulted in a relatively large rate of descent (8 ft/sec) at contact. The airspeed at touchdown was 180 KIAS, and the angle of attack was 7.6°.

Fourth flight (2-3-9).- Shortly after launch on this flight, an in-flight explosion occurred in the engine compartment, which necessitated an emergency landing on an alternate landing site (Rosamond Dry Lake). Again, the roll damper failed at launch.

Figure 13 shows that the flare was initiated at an altitude of about 950 feet with a speed of 253 KIAS. The flare continued to brake the vertical velocity to a point approximately 4 seconds prior to touchdown. At this point, the altitude was slightly greater than 30 feet, the airspeed was 184 KIAS, and the rate of descent was 4 ft/sec. After continuing to decelerate during the last 4 seconds, the airplane

made contact at an airspeed of 161 KIAS, a vertical velocity of 9.5 ft/sec, and an angle of attack of 10.8°. The landing was hard and resulted in major structural damage to the airplane.

In this instance the lack of speed margin at touchdown, which had been experienced in the previous two landings, allowed the pilot no cushion "to feel" for the ground on an unfamiliar and unmarked landing site. Another contributing factor to the severeness of the landing and the damage sustained was the touchdown weight of 15,183 pounds. A limiting rate of sink of 9 ft/sec had been established, based upon a design weight of 11,500 pounds. However, as the airplane fabrication progressed and necessary modifications were incorporated into the design, the basic airplane weight had increased to nearly 14,000 pounds. In addition, the usual quantity of propellant and oxidizer fluids could not be jettisoned because of the steep descending attitude necessary to reach the landing site. All of these factors contributed to the abnormally high landing weight which even further compromised the allowable rate of descent at touchdown (see ref. 6).

Effect of technique.- As was shown in the discussion of the first four flights, most of the early X-15 landing flares were performed with initial airspeeds of about 250 KIAS. At this speed, the pilot found it necessary to prolong the flare until touchdown in order to land with a proper rate of descent and yet not exceed the angle-of-attack limits. Previous experience in simulating X-15 landings (refs. 1 and 2) demonstrated that starting the flare with excess speed gave the pilot a margin for adjustment at the end of the flare. This condition is illustrated in the flare time history of figure 14 for another X-15 pilot making his first flight.

The flare illustrated (fig. 14) was initiated at an altitude of 580 feet and an airspeed of 309 KIAS. It was essentially completed 20 seconds before touchdown at an altitude of 40 feet and an airspeed of 280 KIAS. At this point, it was possible for the pilot to extend the flap and gear without giving undue attention to correcting the induced transient motions. Even after flap and gear extension, the pilot was able to devote almost 10 seconds to the task of further reducing rate of sink and touching down. In this instance, touchdown was accomplished with an airspeed of 174 KIAS, an angle of attack of 7.5°, and a rate of sink of 5 ft/sec.

A comparison of the time history of figure 14 with time histories of the first four flights (figs. 10 to 13) shows that the pilot, by increasing his speed margin, had more than doubled the time available for making a gentle landing. Increasing the speed margin does not, in itself, guarantee that the pilot will make a good landing. But, by increasing the time interval in the presence of the ground, the pilot materially improves his chances of minimizing the rate of sink at

touchdown. He affords himself a finite time interval for estimating his rate of descent, adjusting it as required, and touching down before speed has decayed to a dangerously low value.

Inspection of figure 14 reveals that large stabilizer control inputs were applied during the landing, which suggests a tendency for the pilot to overcontrol. Similar tendencies were observed in the data of reference 14 from which it was determined that some pilots, particularly fighter pilots, derive a more satisfactory "feel" and response from the controls by applying abrupt, rapid stick motions. Other landings by pilot C, a former fighter pilot, exhibited this tendency, which indicates that the cause was one of technique rather than overcontrol.

H
2
2
1

Effect of dampers.- As mentioned previously, lack of pitch damping was considered to be a contributing factor in the oscillations encountered in the first flight. That the lack of roll damping had little effect was also noted in the initial landings. It is of interest, therefore, to consider the results obtained under similar conditions in later flights, particularly those flights made without pitch damping.

A recurrence of inoperative pitch damping took place on flight 1-2-7 in which the damper apparently failed prior to launch. Because of the nature of the failure, however, the pilot was not aware of the trouble. Figure 15 presents a time history of the landing which shows that a preliminary flare was performed by using the center stick at an altitude of 1,860 feet and an airspeed of 279 KIAS while the airplane was turning onto the final approach several thousand feet to the side of the runway centerline. A final flare was then initiated at an altitude slightly less than 500 feet and an airspeed of 270 KIAS. No large oscillations were encountered during this flare, and touchdown was accomplished at an airspeed of 189 KIAS, a rate of sink of 5 ft/sec, and an angle of attack of 7.1°. Although the pilot realized that the airplane did not handle as it had in the previous three flights (because of the damper failure), he had no difficulty in making the landing.

After a number of maneuvers were performed at safe altitudes with all dampers intentionally inoperative, in addition to the earlier landings with pitch- or roll-damper malfunctions, a landing with all dampers off was demonstrated in flight 2-8-16. In this flight the entire flare was made with the pilot using the center stick only. As shown in figure 16, the flare was initiated at an altitude of 630 feet and an airspeed of 270 KIAS. Shortly after the initiation of the flap cycle ($t \approx 16$ sec), a transient motion in roll with a peak roll rate of 13.5 deg/sec occurred. This was the largest roll transient observed during any flare, including that of the glide flight. The transient

was quickly damped, however, and the remainder of the landing was routine. Touchdown conditions were an airspeed of 185 KIAS, a rate of sink of 3.5 ft/sec, and an angle of attack of 6.6°. This landing proved that the X-15 could be landed with all dampers off without encountering the objectionable oscillations experienced on the first flight.

Evaluation of side-stick controller.- Another factor believed to have contributed to the oscillations experienced on the first flight was the sensitivity of the side-stick controller used to perform the flare. With a backlog of experience that included 10 landings in the X-15, pilot A again tested the suitability of the side stick for landing in flight 2-9-18. In this instance, however, the pitch damper was operating. The time history for this flare is shown in figure 17. H 2 2 1

Although no pronounced aircraft oscillations are evident in figure 17, the horizontal-stabilizer and normal-acceleration curves show some overcontrol tendencies throughout the flare. The flare was initiated at an altitude of 464 feet and an airspeed of 282 KIAS. Touchdown was delayed, however, until the comparatively slow speed of 160 KIAS was reached. The angle of attack was 11.2° and the rate of sink was 4 ft/sec at touchdown.

One additional landing (flight 2-10-21) was performed using the side stick. The pilot again had some difficulty in controlling the airplane, particularly near the ground, and conceded at this time that he felt he could perform more satisfactory landings with the less-sensitive center stick. This concession does not necessarily imply that the side-stick controller is unsatisfactory, however. Previous tests at the Flight Research Center using an F-107A airplane equipped with a side controller similar to that used in the X-15 showed that low controller sensitivity for landing may not be an essential requirement. Several of the X-15 pilots flew the F-107A airplane and performed, among other maneuvers, complete landings using only the side stick. After a number of landings were performed, each pilot could land equally well with the side stick and the center stick. Thus, with some experience, good landings can be performed with either means of control.

Effect of flap angle.- The improper flap actuation in the second flight, discussed previously, actually resulted in a comfortable flare from a piloting standpoint. Thus, a reappraisal of available wind-tunnel data was made which showed that, by decreasing the flap travel from 40° to 30°, a reduction in drag and a corresponding increase in lift-drag ratio could be obtained (see figs. 4(c) and 4(d)) without noticeably affecting the angle of attack for landing. Figure 18 is a time history of a flare with the 30°-flap extension (flight 2-7-15). The initial flare was begun about 28 seconds before touchdown from an altitude of about 1,100 feet and an airspeed of 297 KIAS, followed by

a second flare performed shortly after flap actuation. Touchdown conditions were an airspeed of 193 KIAS, angle of attack of 7.1°, and rate of sink of 2.5 ft/sec.

Summary.- Figure 19 presents, in terms of landing speed, a summary of various flare and touchdown parameters, including touchdown angle of attack and vertical velocity, time to perform the flare, and flare-initiation altitude and airspeed. Touchdown statistics and limitations are further summarized in figure 20 and table III. Each factor is briefly discussed in the following sections, and the variations among the different pilots are indicated.

Examination of the data of figure 19 shows that an average X-15 flare would begin at an altitude of about 800 feet and an airspeed of about 300 KIAS. The time required to perform the flare and touchdown is usually less than 30 seconds. Average touchdown conditions are of the order of an airspeed of 185 KIAS, a rate of sink of 4 ft/sec, and an angle of attack of 7°. All the pilots believed that, when the center stick was used, the X-15 could be controlled adequately even with all dampers off.

Angle of attack at touchdown: Figure 19 shows that the angle of attack at touchdown, as expected, generally increases with decreasing touchdown speed. As shown, pilot A, in particular, has landed at slower speeds than the other pilots; hence, the touchdown angles of attack for his flights were higher than average. In general, the angles of attack at touchdown have varied from about 4° at high speeds to near 11° at low speeds. Also shown for reference in this figure is the angle of attack for 1 g trim flight with a wing loading of 73 lb/sq ft. Since most of the touchdowns have been made near 1 g, the lower trend in angle of attack shown for the flight data is attributed to ground effects.

Vertical velocity at touchdown: This parameter, with rates extending to 9.5 ft/sec (fig. 19), seems to be relatively independent of touchdown speed. The average rate of sink at touchdown of about 4 ft/sec is somewhat higher than that reported in reference 12.

Time to complete flare: The time interval from flare initiation to touchdown also appears to be independent of touchdown speed; for this investigation the average time is about 27 seconds.

Airspeed at flare initiation: This parameter generally increases with increasing touchdown speed, as might be expected. It is interesting to note, however, that the flares starting from the highest speed (V_i = 339 KIAS on flight 1-15-28) and the lowest speed (V_i = 242 KIAS on flight 2-1-3) both terminate at touchdown airspeeds slightly below the average of approximately 185 KIAS.

Altitude at flare initiation: A generally diminishing trend with decreasing airspeed is noted for this altitude in figure 19. There is, however, a wide spread in the results arising from differences in flare abruptness and the point of gear and flap extension.

Touchdown dispersion: In a number of flights, pilots B to G have attempted to touch down at preselected points on the landing runway. Table III summarizes the dispersions from these preselected points. Three touchdowns occurred over 2,000 feet from the intended point, and three others extended just beyond 1,000 feet; whereas, in five of the more recent landings, contact was made in less than 1,000 feet. Excluding some of the early attempts, these data verify the conclusion of reference 1 that landings of the X-15 should be possible within ±1,000 feet of a designated point.

Gear design envelope: Figure 20 presents the gear design envelope defined by touchdown angle of attack and vertical velocity. This envelope actually imposed a rather severe task on the pilot in executing the flare so that the touchdown limitations would not be exceeded. The dashed line shows the original design limit (based upon a design weight of 11,500 lb) applicable to the first four landings designated by the solid symbols. It can be seen that the first three landings closely approached the limit, and that the fourth considerably exceeded the limit. As noted before, major structural damage was incurred on this landing (flight 2-3-4). Reference 6 describes in detail the manner in which the gear was strengthened, thereby raising the limits to the present levels (based upon a design weight of 14,500 lb) indicated by the solid lines. All subsequent landings were within the new limits, although two landings made by pilot A were very close to these limits.

Value of In-Flight Simulation

Prior to and during the X-15 flight program, numerous in-flight landing simulations have been performed using, primarily, F-104 airplanes. Fixed-base simulations served concurrently as a guide for determining the range of control parameters which should be investigated. Because the visual cues and motion stimuli of flight were lacking, however, the fixed-base simulations did not provide an adequate sense of realism. For the in-flight simulation the Flight Research Center and the Air Force Flight Test Center used F-104 airplanes and North American Aviation used an F-100A. Both airplanes approximated the X-15 wing loading.

Performance data from the F-104A tests, reported in reference 2, are shown with X-15 data in figure 21. As can be seen, when appropriate combinations of extended gear, flaps, and speed brakes are used, the F-104A at zero thrust should be able to simulate the X-15 well.

The ability of the F-104 to simulate the X-15 is more convincingly demonstrated in figure 22, which shows the good correlation between an F-104 flight pattern and the X-15 predicted landing pattern previously presented in figure 7. Also included is a similar pattern for the F-100A airplane used by the manufacturer with idle engine power, extended gear, speed brake, and a drag parachute. Both of these vehicles enabled the pilots in simulated X-15 landings to establish geographic check points and key altitudes around the pattern; thus, they became familiar with the precise timing required in the pattern by the low lift-drag ratio. Even the X-15 flare characteristics were well represented by the F-104A, as can be seen in figure 23. Speeds, vertical velocities, altitudes, and normal acceleration correlated well, which provided the pilot with the proper motion stimuli and visual cues. The results from the fixed-base analog simulation are included for comparison.

At present, prior to each X-15 flight, the pilot devotes an entire F-104 flight to simulated approaches and flares. The pilots all readily agree on the value of these flight simulations (ref. 15) and feel that such procedures should be seriously considered for all future reentry gliders having low lift-drag ratios.

CONCLUDING REMARKS

This analysis of the first 30 landing approach and flare maneuvers made with the X-15 airplane provides a useful background of flight experience and a relatively good cross section of landing characteristics applicable to future low-lift-drag-ratio gliders. Seven X-15 pilots, after a suitable period of indoctrination, have now flown the aircraft. Among the significant results from these early X-15 flights are the following items:

Analysis of the flight data indicates that the peak lift-drag ratio for the X-15 at landing speeds varied between 3.5 and 4.5, depending on configuration, and was somewhat higher than predicted. In this range of lift-drag ratios the pilots were able to establish a fairly wide range of easily controlled approach patterns and flares without devoting undue attention to space position, pattern speeds, or sinking rates.

In spiral-type overhead patterns starting from altitudes as high as 40,000 feet, the pilots, through the use of speed-brake modulation and maneuvering flight, were able to define a "gate" on the downwind leg of the pattern having ±8,000-foot altitude deviations and ±10,000-foot lateral deviations and yet touch down consistently within about ±1,000 feet of a preselected point.

The flare was found to be the most problematical phase of the X-15 landings, largely because of the relatively severe touchdown angle-of-attack limitations imposed by the landing-gear design. In the landing evaluation, most of the airplane deficiencies and piloting problems emerged during the flare maneuvers of the first four landings. Thereafter, the task became easier.

A typical flare was initiated at a "comfortable" altitude of about 800 feet and an indicated airspeed of approximately 300 knots, which allowed a margin of excess speed. When the flare was essentially completed, the flap and gear were extended, thus delaying to the last possible moment the rapid speed decay associated with the low lift-drag ratios and allowing the pilot additional time for final adjustments. Average touchdowns have been accomplished at speeds of about 185 KIAS with angles of attack of about 7° and rates of sink of about 4 ft/sec.

All the pilots believed that, when the center stick was used, the X-15 could be controlled adequately even with all dampers off.

The extensive fixed-base and flight simulations, particularly those made with the F-104 airplanes, were accurate and valuable aids in this landing program.

Flight Research Center,
National Aeronautics and Space Administration,
Edwards, Calif., April 12, 1961

REFERENCES

1. Weil, Joseph, and Matranga, Gene J.: Review of Techniques Applicable to the Recovery of Lifting Hypervelocity Vehicles. NASA TM X-334, 1960.

2. Matranga, Gene J., and Armstrong, Neil A.: Approach and Landing Investigation at Lift-Drag Ratios of 2 to 4 Utilizing a Straight-Wing Fighter Airplane. NASA TM X-31, 1959.

3. Matranga, Gene J., and Menard, Joseph A.: Approach and Landing Investigation at Lift-Drag Ratios of 3 to 4 Utilizing a Delta-Wing Interceptor Airplane. NASA TM X-125, 1959.

4. Finch, Thomas W., and Matranga, Gene J.: Launch, Low-Speed, and Landing Characteristics Determined From the First Flight of the North American X-15 Research Airplane. NASA TM X-195, 1959.

5. Flight Research Center: Aerodynamic and Landing Measurements Obtained During the First Powered Flight of the North American X-15 Research Airplane. NASA TM X-269, 1960.

6. McKay, James M., and Scott, Betty J.: Landing-Gear Behavior During Touchdown and Runout for 17 Landings of the X-15 Research Airplane. NASA TM X-518, 1961.

7. Stillwell, Wendell H., and Larson, Terry J.: Measurement of the Maximum Speed Attained by the X-15 Airplane Powered With Interim Rocket Engines. NASA TN D-615, 1960.

8. Dreher, Robert C.: An Airborne Indicator for Measuring Vertical Velocity of Airplanes at Wheel Contact. NACA TN 2906, 1953.

9. Saltzman, Edwin J.: Preliminary Full-Scale Power-Off Drag of the X-15 Airplane for Mach Numbers From 0.7 to 3.1. NASA TM X-430, 1960.

10. Breuhaus, W. O., Reynolds, P. A., and Kidd, E. A.: Handling Qualities Requirements for Hyper-Velocity Aircraft. Rep. No. TC-1332-F-1, Cornell Aero. Lab., Inc., Sept. 30, 1959 (rev. Jan. 28, 1960).

11. Bray, Richard S., Drinkwater, Fred J., III, and White, Maurice D.: A Flight Study of a Power-Off Landing Technique Applicable to Re-Entry Vehicles. NASA TN D-323, 1960.

12. Stillwell, Wendell H.: Results of Measurements Made During the Approach and Landing of Seven High-Speed Research Airplanes. NACA RM H54K24, 1955.

13. Crossfield, A. Scott, and Blair, Clay, Jr.: Always Another Dawn. The World Publishing Co., 1960, pp. 343-344.

14. Pembo, Chris, and Matranga, Gene J.: Control Deflections, Airplane Response, and Tail Loads Measured on an F-100A Airplane in Service Operational Flying. NACA RM H58C26, 1958.

15. White, Robert M., and Walker, Joseph A.: Pilots Report on X-15 Flight Tests. Space/Aeronautics, vol. 35, no. 2, Feb. 1961, pp. 55-58.

TABLE I.- PHYSICAL CHARACTERISTICS OF THE X-15 AIRPLANE

Wing:	
Airfoil section	NACA 66005 (Modified)
Total area (includes 94.98 sq ft covered by fuselage), sq ft	200
Span, ft	22.36
Mean aerodynamic chord, ft	10.27
Root chord, ft	14.91
Tip chord, ft	2.98
Taper ratio	0.20
Aspect ratio	2.50
Sweep at 25-percent-chord line, deg	25.64
Incidence, deg	0
Dihedral, deg	0
Aerodynamic twist, deg	0
Flap -	
Type	Plain
Area (each), sq ft	8.30
Span (each), ft	4.50
Inboard chord, ft	2.61
Outboard chord, ft	1.08
Deflection, down, deg	See table III
Ratio flap chord to wing chord	0.22
Ratio total flap area to wing area	0.08
Ratio flap span to wing semispan	0.40
Trailing-edge angle, deg	5.67
Sweepback angle of hinge line, deg	0
Horizontal tail:	
Airfoil section	NACA 66005 (Modified)
Total area (includes 63.29 sq ft covered by fuselage), sq ft	115.34
Span, ft	18.08
Mean aerodynamic chord, ft	7.05
Root chord, ft	10.22
Tip chord, ft	2.11
Taper ratio	0.21
Aspect ratio	2.83
Sweep at 25-percent-chord line, deg	45
Dihedral, deg	-15
Ratio horizontal-tail area to wing area	0.58
Movable surface area, sq ft	51.77
Deflection -	
Longitudinal, up, deg	15
Longitudinal, down, deg	35
Lateral differential (pilot authority), deg	±15
Lateral differential (autopilot authority), deg	±30
Control system. .	Irreversible hydraulic boost with artificial feel

TABLE I.- PHYSICAL CHARACTERISTICS OF THE X-15 AIRPLANE - Concluded

Upper vertical tail:	
Airfoil section	10° single wedge
Total area, sq ft	40.91
Span, ft	4.58
Mean aerodynamic chord, ft	8.95
Root chord, ft	10.21
Tip chord, ft	7.56
Taper ratio	0.74
Aspect ratio	0.51
Sweep at 25-percent-chord line, deg	23.41
Ratio vertical-tail area to wing area	0.20
Movable surface area, sq ft	26.45
Deflection, deg	±7.50
Sweepback of hinge line, deg	0
Control system. .	Irreversible hydraulic boost with artificial feel
Lower vertical tail:	
Airfoil section	10° single wedge
Total area, sq ft	34.41
Span, ft	3.83
Mean aerodynamic chord, ft	9.17
Root chord, ft	10.21
Tip chord, ft	8
Taper ratio	0.78
Aspect ratio	0.43
Sweep at 25-percent-chord line, deg	23.41
Ratio vertical-tail area to wing area	0.17
Movable surface area, sq ft	19.95
Deflection, deg	±7.50
Sweepback of hinge line, deg	0
Control system. .	Irreversible hydraulic boost with artificial feel
Fuselage:	
Length, ft	50.75
Maximum width, ft	7.33
Maximum depth, ft	4.67
Maximum depth over canopy, ft	4.97
Side area (total), sq ft	215.66
Fineness ratio	10.91
Speed brake (typical for each of four):	
Area, sq ft	5.57
Span, ft	1.67
Chord, ft	3.33
Deflection, deg	35

TABLE II.- CHARACTERISTICS OF X-15 STABILITY AUGMENTATION SYSTEM

Damper setting	Gain							
	Pitch		Roll		Yaw		Yar	
	In/deg/sec	Deg/deg/sec	In/deg/sec	Deg/deg/sec	In/deg/sec	Deg/deg/sec	In/deg/sec	Deg/deg/sec
1	0.005	0.075	0.0017	0.051	0.004	0.03	0.003	0.09
2	.010	.150	.0033	.100	.008	.06	.006	.18
3	.015	.225	.0050	.150	.012	.09	.009	.27
4	.020	.300	.0067	.200	.016	.12	.012	.36
5	.025	.375	.0083	.250	.020	.15	.015	.45
6	.030	.450	.0100	.300	.024	.18	.018	.54
7	.035	.525	.0117	.350	.028	.21	.021	.63
8	.040	.600	.0134	.400	.032	.24	.024	.72
9	.045	.675	.0150	.450	.036	.27	.027	.81
10	.050	.750	.0167	.500	.040	.30	.030	.90
Condition	Servo and surface limits							
Normal functioning	Maximum servo-actuator travel = ±1.0 inch or ±15° of horizontal stabilizer		Maximum servo-actuator travel = ±1.0 inch or ±15° of horizontal stabilizer		Maximum servo-actuator travel = ±1.0 inch or ±7.5° of vertical stabilizer		Maximum servo-actuator travel = ±1.0 inch or ±15° of horizontal stabilizer	
Mal-functioning	0.1 inch or 1.5° of horizontal stabilizer		0.1 inch or 3° of differential stabilizer		0.1 inch or 0.75° of vertical stabilizer		0.1 inch or 3° of differential stabilizer	

TABLE III.- SUMMARY OF X-15 LANDING DATA

Flight	Pilot	W, lb	Damper setting	Stick	Pattern									
					Type	h_{180}, ft	$V_{i_{180}}$, knots	x_{180}, ft	y_{180}, ft	h_{90}, ft	$V_{i_{90}}$, knots	x_{90}, ft	y_{90}, ft
1-1-5	A	13,234	0-2-8	Side	S	10,163	247	10,654	20,383	5,068	270	22,272	10,565
2-1-3	A	13,984	2-4-8	Center	S	10,230	253	5,442	17,264	4,210	282	19,867	6,210
2-2-6	A	14,165	2-0-8	Center	S	10,330	276	5,330	20,650	6,160	246	19,470	11,890
2-3-9	A	15,183	2-0-8	Center	270°	9,820	250	8,250	17,480	4,720	265	19,730	6,500
1-2-7	A	13,988	0-4-8	Center	270°	------	-----	------	------	3,700	276	16,007	8,522
2-4-11	A	15,062	2-4-8	Center	270°	12,880	332	-2,451	23,940	4,040	300	18,390	9,510
2-5-12	A	14,798	2-4-8	Center	360°	12,300	260	11,909	20,422	5,711	311	22,791	10,295
2-6-13	A	14,619	4-4-8	Center	270°	10,102	-----	4,176	23,907	4,740	-----	18,471	11,058
1-3-8	B	14,564	4-0-8	Center	180°	------	-----	------	------	------	-----	------	------
2-7-15	A	14,394	4-4-8	Center	360°	9,445	279	7,300	20,122	4,731	274	17,573	9,820
2-8-16	A	14,583	0-0-0	Center	360°	11,140	296	-5,650	21,022	3,788	271	16,020	9,100
1-4-9	C	14,641	4-4-8	Center	180°	13,771	-----	12,844	18,121	6,430	331	28,120	5,286
1-5-10	B	14,610	4-4-8	Center	270°	7,782	281	8,401	15,530	3,862	296	13,990	8,019
1-6-11	C	14,233	4-0-8	Center	180°	15,980	328	8,718	18,244	6,625	338	25,904	7,560
1-7-12	B	14,790	4-4-8	Center	270°	14,124	300	3,103	22,141	6,855	309	22,572	11,958
1-8-13	C	14,444	4-4-8	Center	180°	14,538	305	0	23,766	4,766	300	20,041	5,500
2-9-18	A	14,469	4-4-8	Side	360°	11,291	275	7,027	28,184	4,624	270	21,524	8,689
1-9-17	B	14,838	4-4-8	Center	270°	10,142	306	11,500	16,075	5,495	325	19,636	9,233
1-10-19	C	14,318	4-4-8	Center	270°	10,595	310	13,281	15,107	4,958	320	21,401	4,325
1-11-21	B	14,411	4-4-8	Center	270°	11,015	304	13,968	13,557	5,320	330	20,378	5,513
1-12-23	C	14,758	4-4-8	Center	270°	24,186	324	4,630	31,282	9,380	334	30,885	5,533
1-13-25	D	14,859	4-4-8	Center	360°	13,430	287	22,885	16,920	9,215	295	29,442	9,432
1-14-27	D	14,601	4-4-8	Center	S	25,293	263	0	27,286	12,394	294	34,386	11,463
1-15-28	E	14,670	4-4-8	Center	S	------	-----	------	------	------	-----	------	------
1-16-29	F	14,450	4-4-8	Center	S	16,690	295	0	26,299	5,112	335	20,818	6,580
2-10-21	A	14,419	2-4-8	Side	270°	9,442	254	5,478	21,280	3,952	267	16,995	8,683
1-17-30	F	14,584	4-4-8	Center	180°	18,183	305	0	34,244	8,240	325	24,571	13,376
2-11-22	A	14,486	2-4-8	Center	360°	10,056	317	-2,290	19,255	3,479	288	13,878	8,022
1-18-31	G	14,559	4-4-8	Center	270°	25,190	265	702	31,378	8,825	321	27,831	10,301
2-12-23	A	14,381	2-4-8	Center	270°	10,163	323	346	19,576	4,159	297	15,300	8,744

Flight	Pilot	W, lb	Damper setting	Stick	Flare initiation																
					Flare and touchdown					Flap extension				Gear extension			Touchdown				
					h_f, ft	V_{i_f}, knots	V_{v_f}, fps	Δt_f, sec	$a_{n_{max}}$, g	h_{f_e}, ft	$V_{i_{f_e}}$, knots	Δt_{f_e}, sec	$\delta_{f_{TD}}$, deg	h_{g_e}, ft	$V_{i_{g_e}}$, knots	Δt_{g_e}, sec	$V_{i_{TD}}$, knots	$V_{v_{TD}}$, fps	α_{TD}, deg	Δx, ft	Runway	Wind velocity, knots	Wind direction
1-1-5	A	13,234	0-2-8	Side	1,591	270	-137	33	2.24	698	266	25	38.0	121	223	12	153	-2.0	8.5	------	1	Calm	---------
2-1-3	A	13,984	2-4-8	Center	516	242	-66	15	1.65	324	239	12	23.2	295	240	11	184	-4.0	8.1	------	1	9	SW
[illegible]																						Calm	---------
2-3-9	A	15,183	2-0-8	Center	952	253	-84	29	1.30	379	250	20	37.2	89	220	10	161	-9.5	10.8	------	*Emergency	18	NW
1-2-7	A	13,988	0-4-8	Center	1,860	279	-151	33	1.65	247	262	16	38.0	32	227	7	189	-5.0	7.1	------	2	Calm	---------
2-4-11	A	15,062	2-4-8	Center	1,430	300	-140	35	2.00	186	272	19	33.8	20	218	6	188	-6.5	6.2	------	1	4	SW
2-5-12	A	14,798	2-4-8	Center	1,457	305	-167	40	1.49	65	292	22	32.3	27	217	6	185	-3.5	8.7	------	2	Calm	---------
2-6-13	A	14,619	4-4-8	Center	717	300	-112	23	1.65	380	291	19	33.8	55	257	11	192	-2.5	6.3	------	2	9	NNW
1-3-8	B	14,564	4-0-8	Center	1,200	326	-150	26	1.52	560	317	20	41.9	97	262	8	214	-6.5	4.7	------	1	21	SW
2-7-15	A	14,394	4-4-8	Center	1,108	297	-126	28	1.43	410	288	21	31.5	32	248	10	193	-2.5	7.1	------	2	Calm	---------
2-8-16	A	14,583	0-0-0	Center	630	270	-92	21	1.63	350	266	18	27.2	33	227	7	185	-3.5	6.6	------	2	Calm	---------
1-4-9	C	14,641	4-4-8	Center	579	309	-112	29	1.94	40	288	20	42.3	62	237	11	174	-5.0	7.5	-1,380	1	Calm	---------
1-5-10	B	14,610	4-4-8	Center	555	283	-115	22	1.89	48	278	21	42.5	48	224	7	180	-4.5	7.5	------	3	18	SW
1-6-11	C	14,233	4-0-8	Center	857	316	-104	27	1.55	190	288	20	28.5	35	236	9	189	-1.0	7.4	2,250	1	Calm	---------
1-7-12	B	14,790	4-4-8	Center	851	306	-123	26	1.73	657	305	24	28.7	75	268	12	193	-1.0	5.2	-2,110	2	23	WSW
1-8-13	C	14,444	4-4-8	Center	364	292	-78	26	1.53	80	274	21	29.6	37	225	10	173	-4.5	7.7	2,070	2	19	NNW
2-9-18	A	14,469	4-4-8	Side	464	282	-81	29	1.64	74	254	20	26.5	49	215	11	160	-4.0	11.2	------	2	Calm	---------
1-9-17	B	14,838	4-4-8	Center	868	316	-163	29	2.44	378	299	24	30.0	93	256	13	185	-2.0	7.3	-280	2	7	S
1-10-19	C	14,318	4-4-8	Center	640	323	-113	28	1.86	160	303	21	28.7	33	248	9	198	-1.5	6.1	1,120	2	4	S
1-11-21	B	14,411	4-4-8	Center	725	334	-165	26	2.34	806	334	27	28.6	69	285	15	192	-3.0	5.7	340	2	Calm	---------
1-12-23	C	14,758	4-4-8	Center	1,101	306	-134	33	1.66	108	285	21	29.1	59	240	11	181	-3.5	7.5	-410	2	Calm	---------
1-13-25	D	14,859	4-4-8	Center	1,108	337	-138	26	1.62	1,345	338	28	30.2	556	321	21	196	-4.5	5.7	------	2	Calm	---------
1-14-27	D	14,601	4-4-8	Center	1,214	327	-140	33	1.75	743	321	29	28.1	196	274	17	180	-5.5	7.2	------	1	5	E
1-15-28	E	14,670	4-4-8	Center	919	339	-140	30	1.95	947	339	30	29.2	100	261	14	182	-4.0	7.8	-600	1	Calm	---------
1-16-29	F	14,450	4-4-8	Center	838	316	-137	28	1.80	122	300	19	25.7	47	255	9	195	-2.5	5.4	------	1	19	ENE
2-10-21	A	14,419	2-4-8	Side	268	254	-90	21	1.78	96	250	19	29.7	35	194	8	156	-5.0	10.7	------	2	5	NE
1-17-30	F	14,584	4-4-8	Center	783	312	-121	23	1.51	255	301	18	28.9	37	257	8	209	-4.5	4.4	-630	1	3	N
2-11-22	A	14,486	2-4-8	Center	481	263	-78	17	1.38	390	260	16	27.8	33	226	6	187	-4.0	5.5	------	2	Calm	---------
1-18-31	G	14,559	4-4-8	Center	741	292	-97	26	1.52	780	293	26	28.0	108	246	12	176	-1.5	7.5	-1,116	2	Calm	---------
2-12-23	A	14,381	2-4-8	Center	484	272	-103	20	1.55	244	269	18	27.6	35	213	6	181	-5.5	6.3	------	2	17	NE

*Landing made on Rosamond Dry Lake.

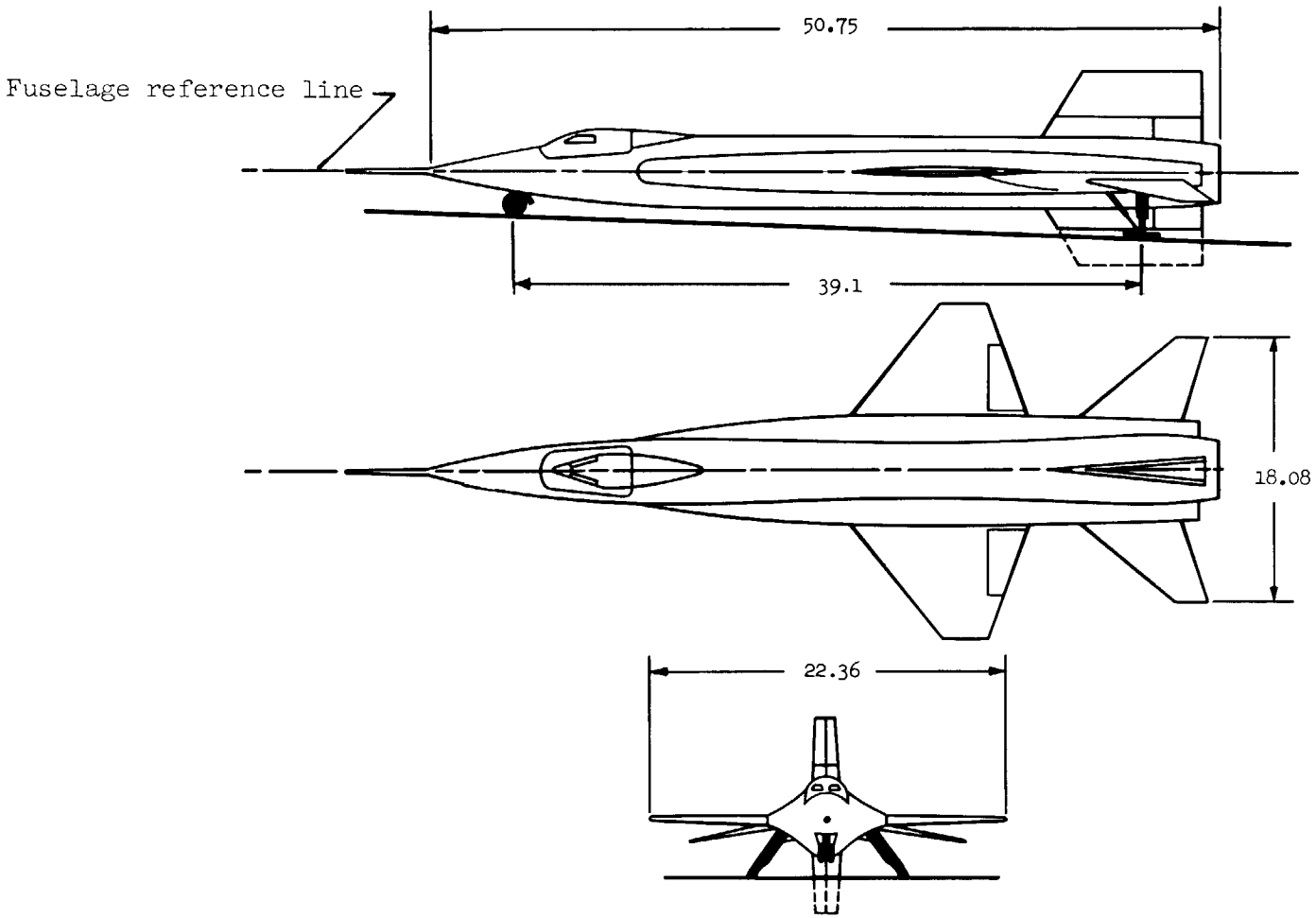

Figure 1.- Three-view drawing of the X-15 airplane. All dimensions in feet.

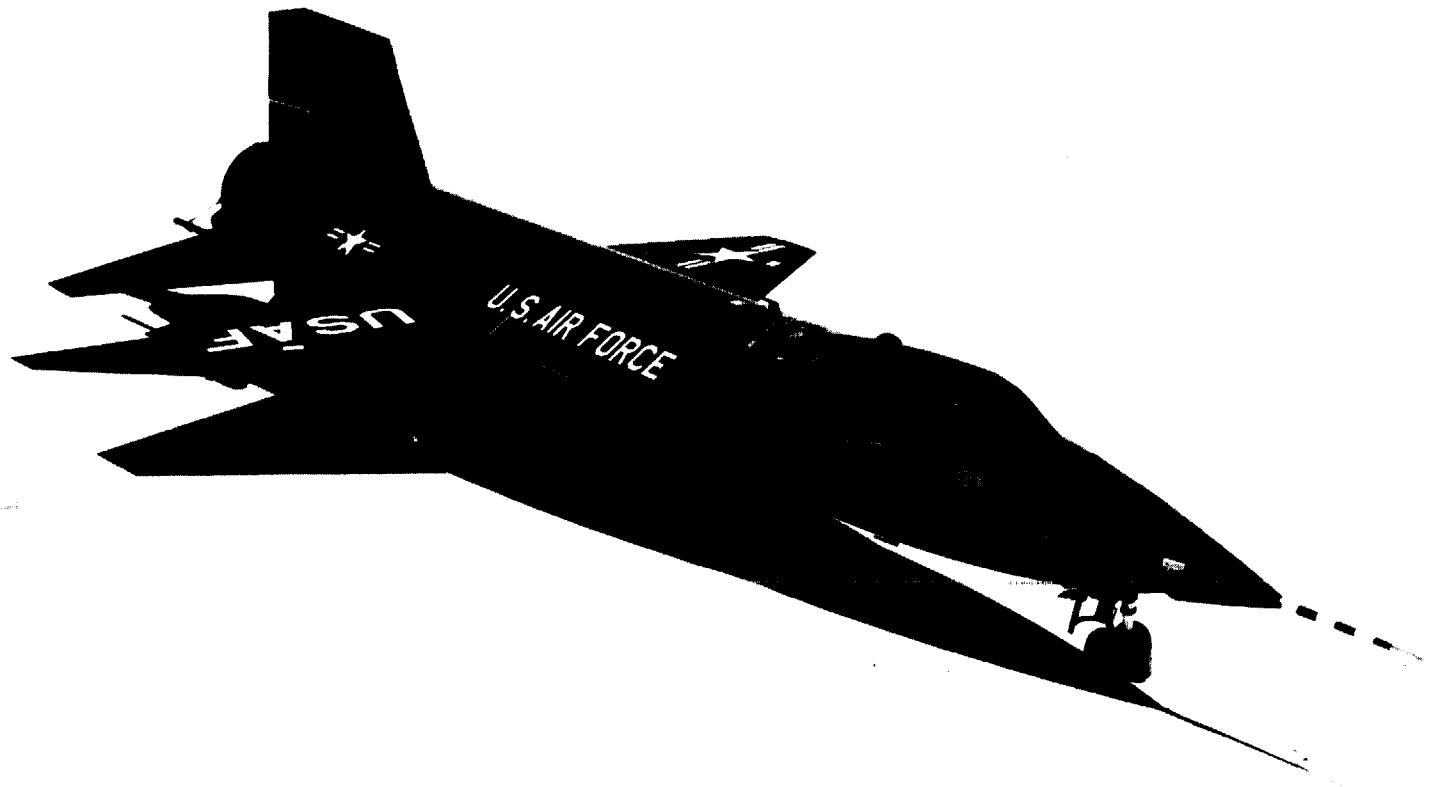

(a) In normal ground attitude. E-5250

Figure 2.- Photograph of the X-15 airplane.

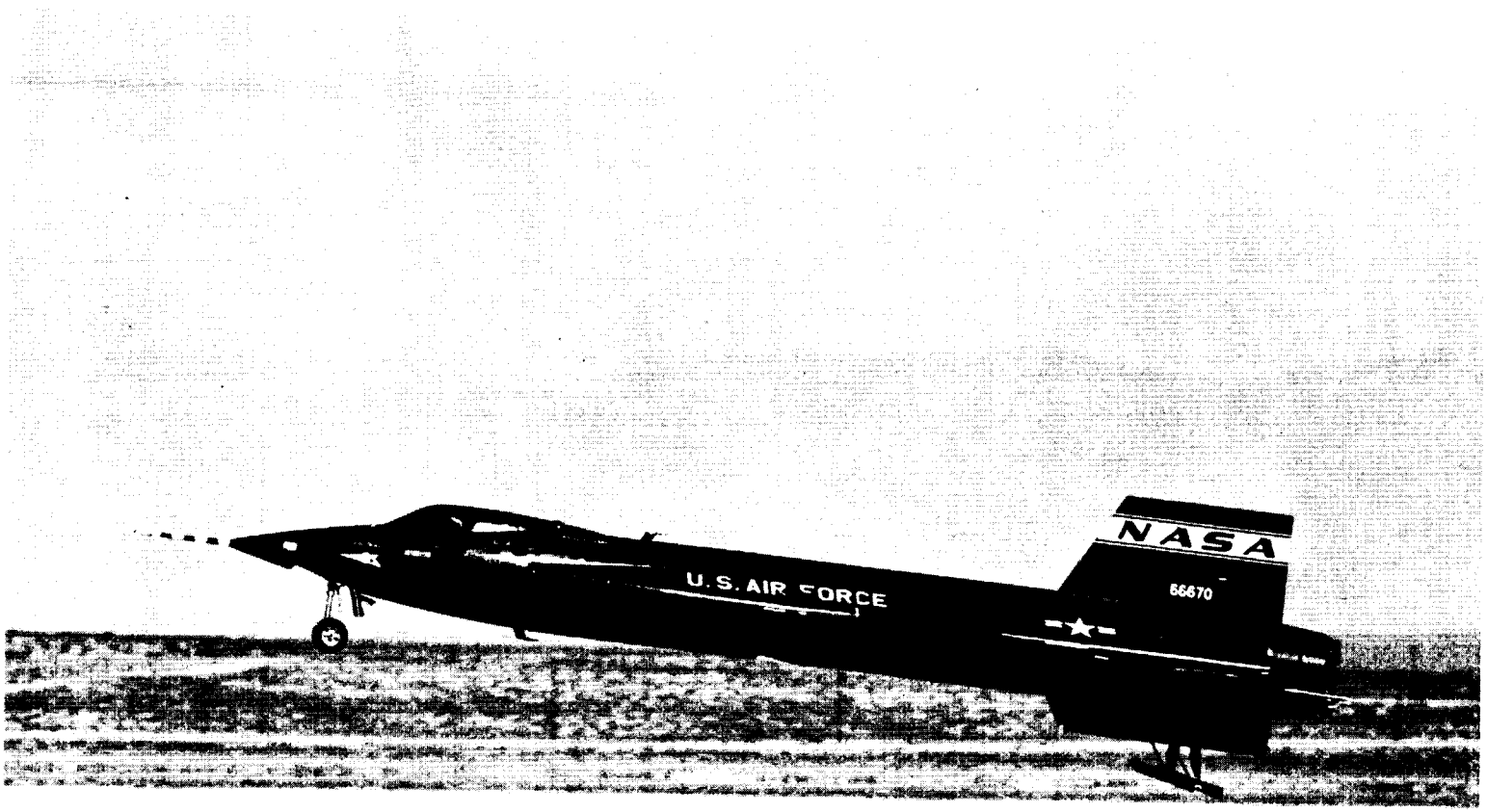

(b) Just prior to main-gear touchdown.

Figure 2.- Concluded.

Figure 3.- Photograph of Rogers Dry Lake. Runways denoted by numbers. E-6419

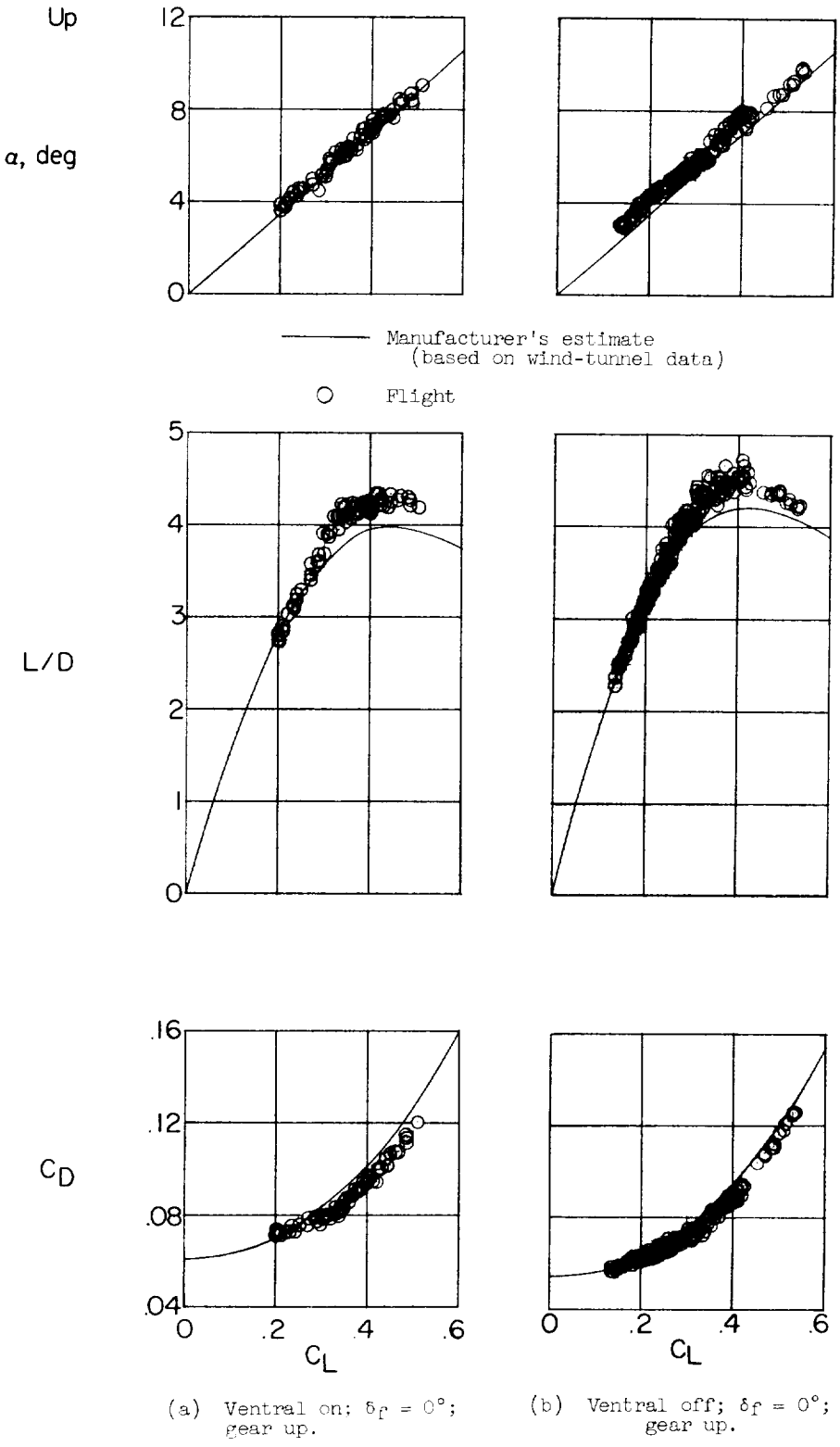

(a) Ventral on; $\delta_f = 0°$; gear up.

(b) Ventral off; $\delta_f = 0°$; gear up.

Figure 4.- X-15 performance data measured during the approach and landing.

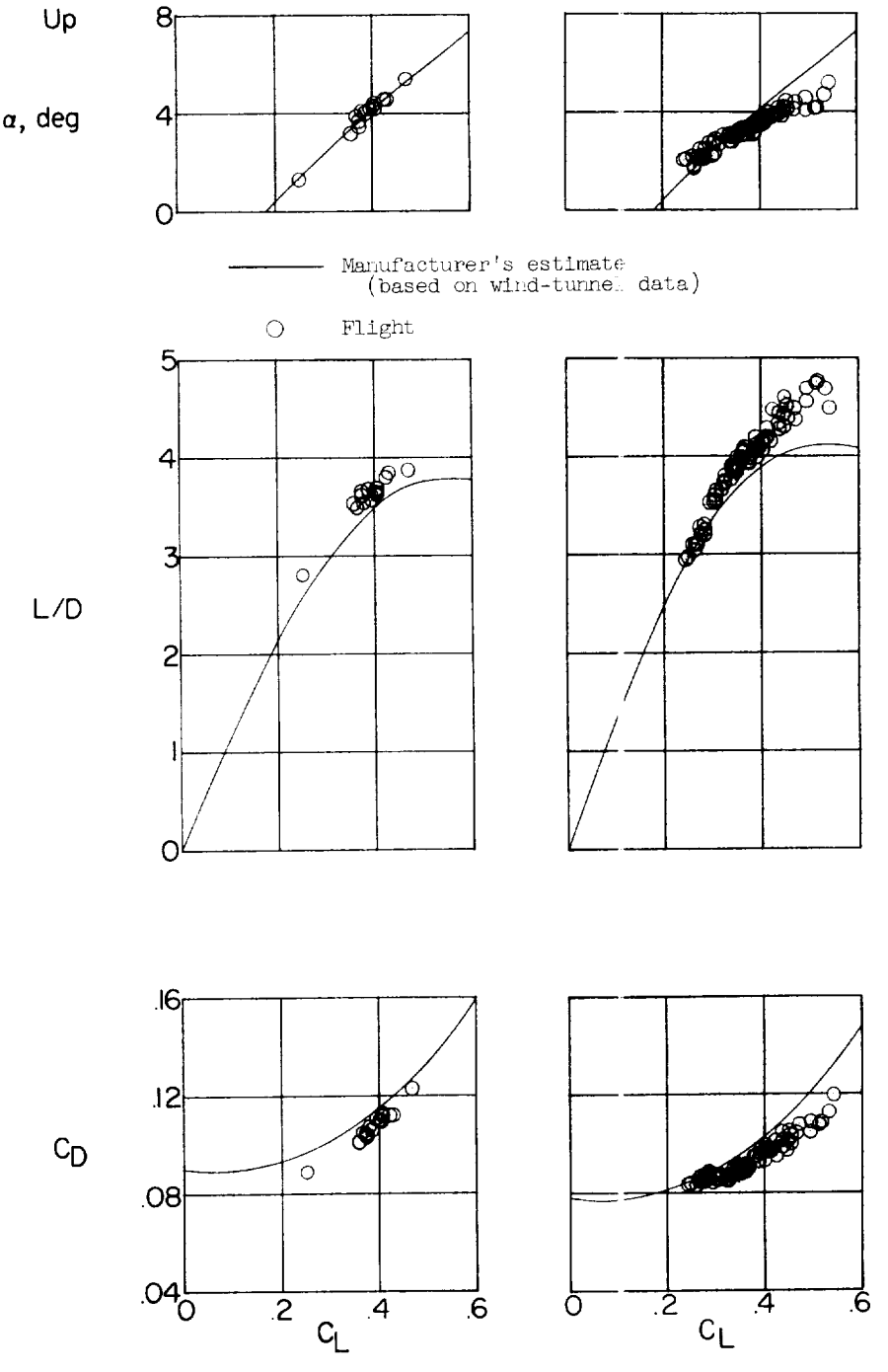

(c) Ventral off; δ_f = 40°; gear up.

(d) Ventral off; δ_f = 30°; gear up.

Figure 4.- Continued.

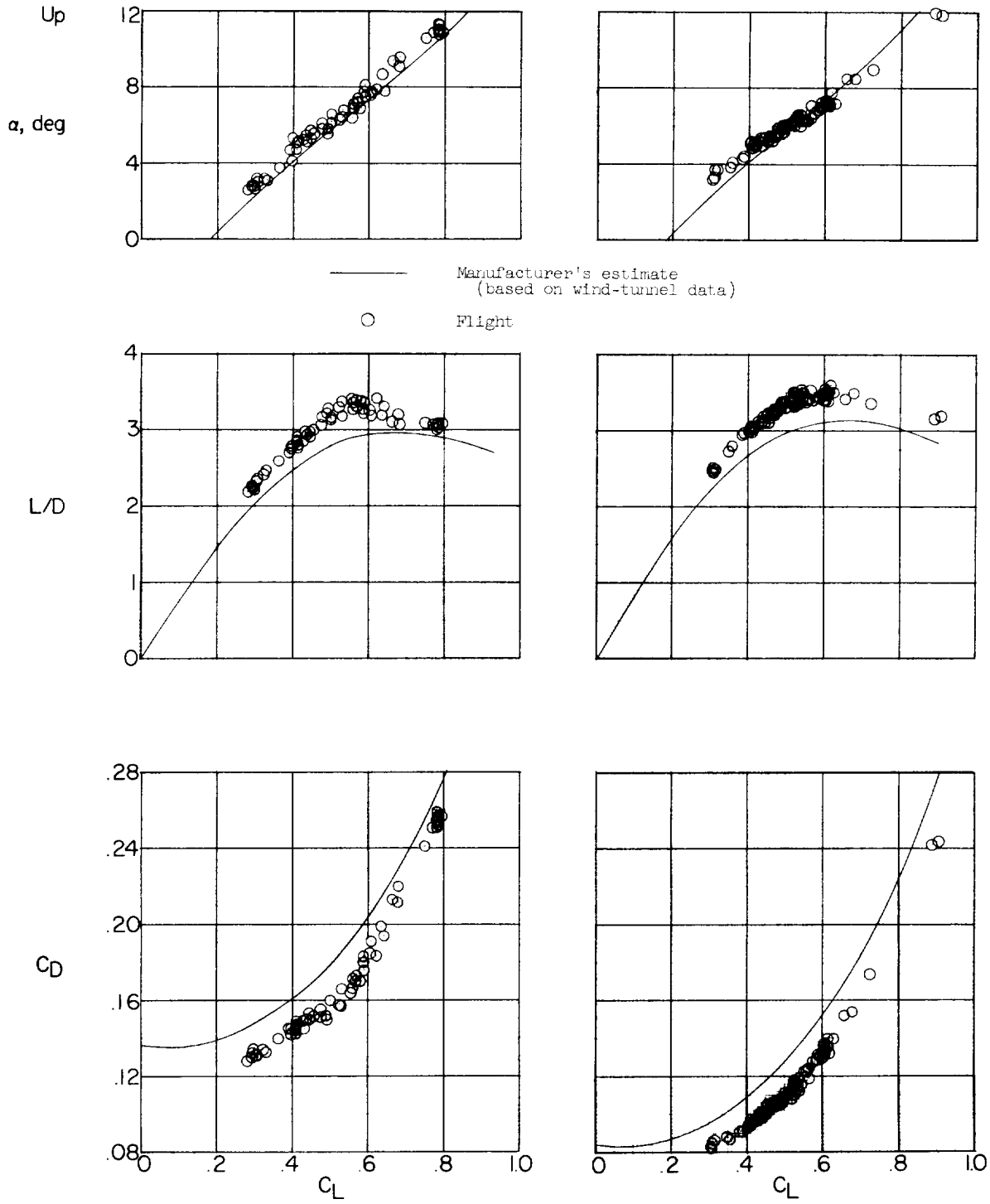

(e) Ventral off; δ_f = 40°; gear extended.

(f) Ventral off; δ_f = 30°; gear extended.

Figure 4.- Concluded.

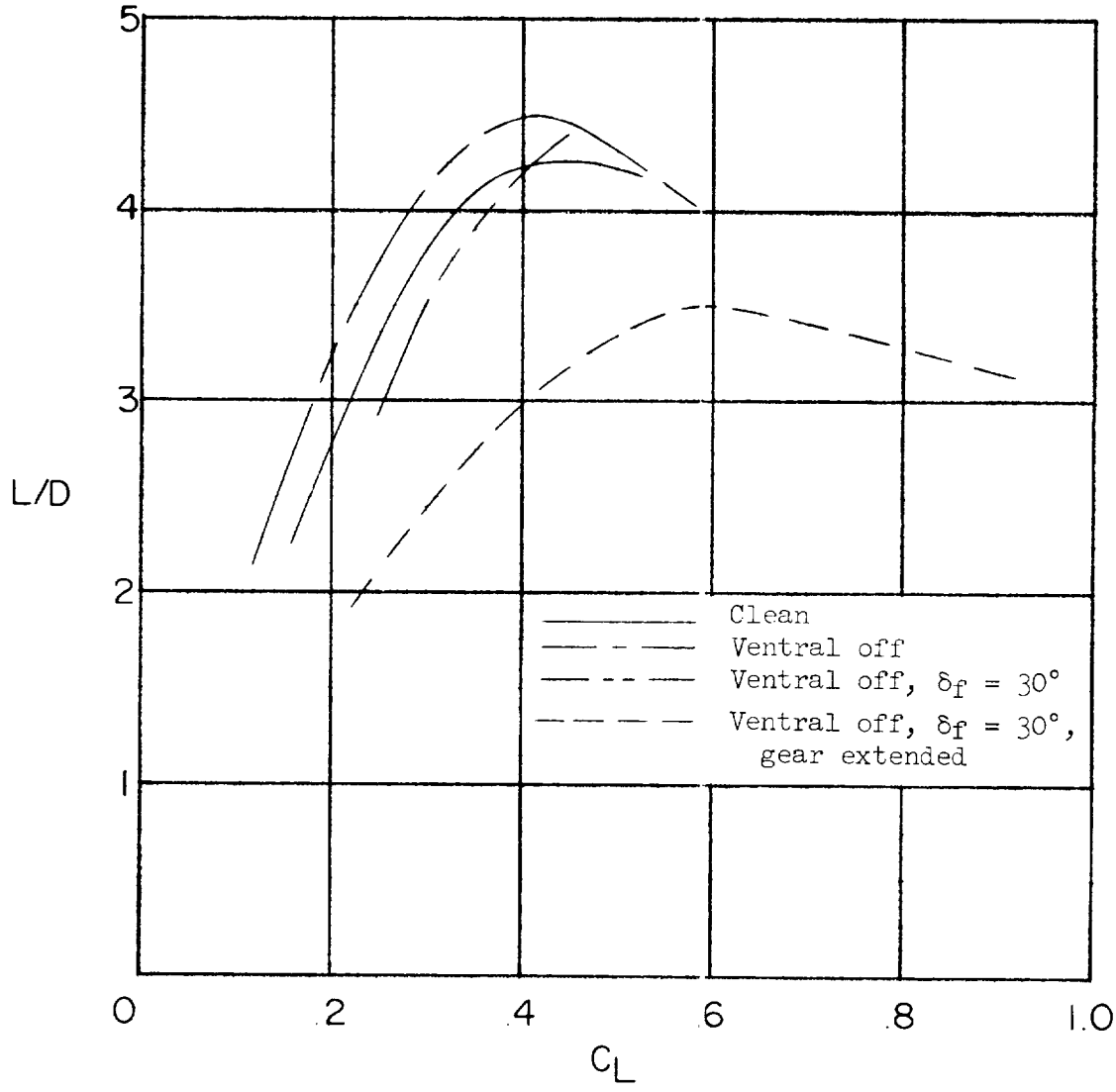

Figure 5.- Flight-measured lift-drag ratio as a function of lift coefficient for various X-15 approach and landing configurations.

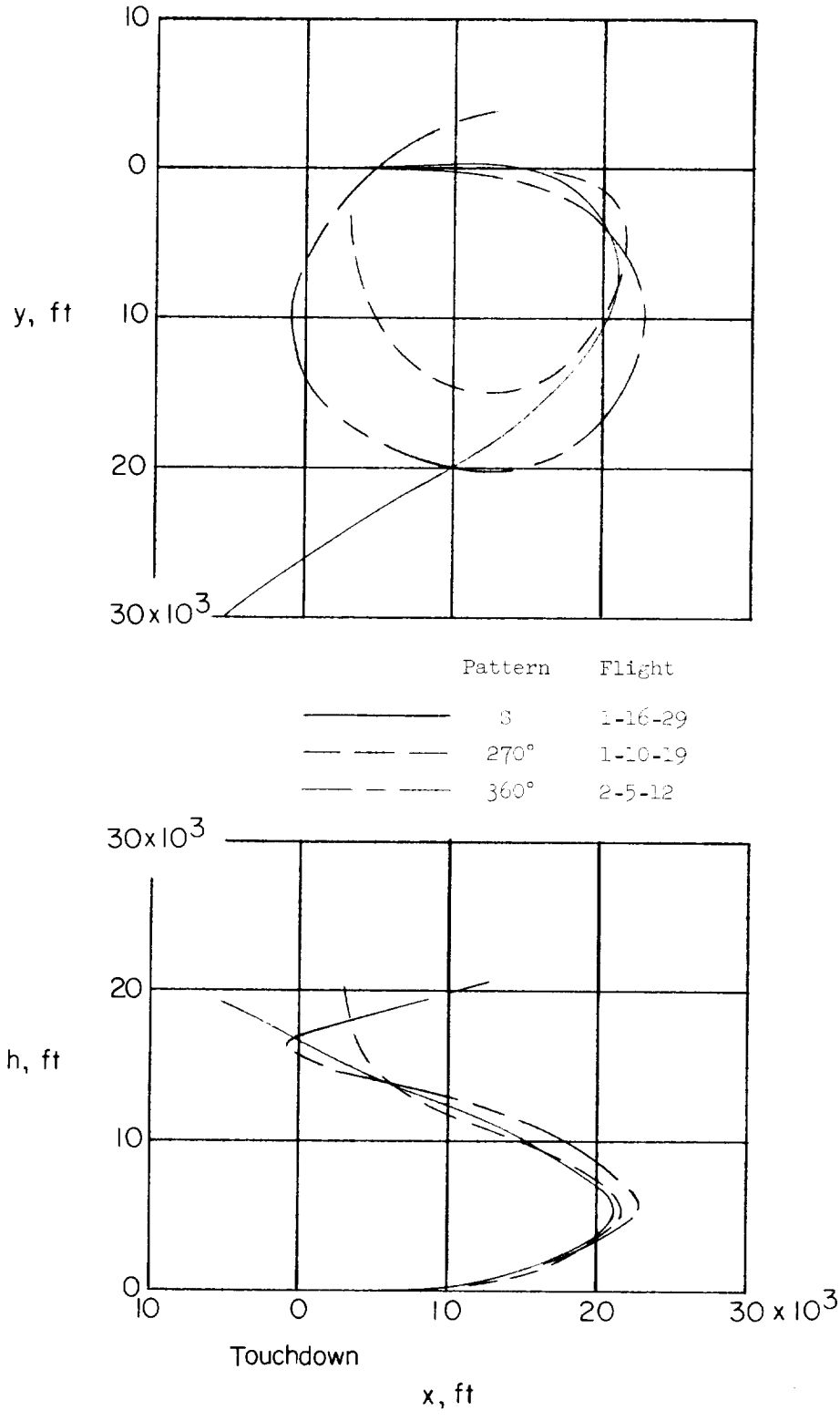

Figure 6.- Representative X-15 landing patterns.

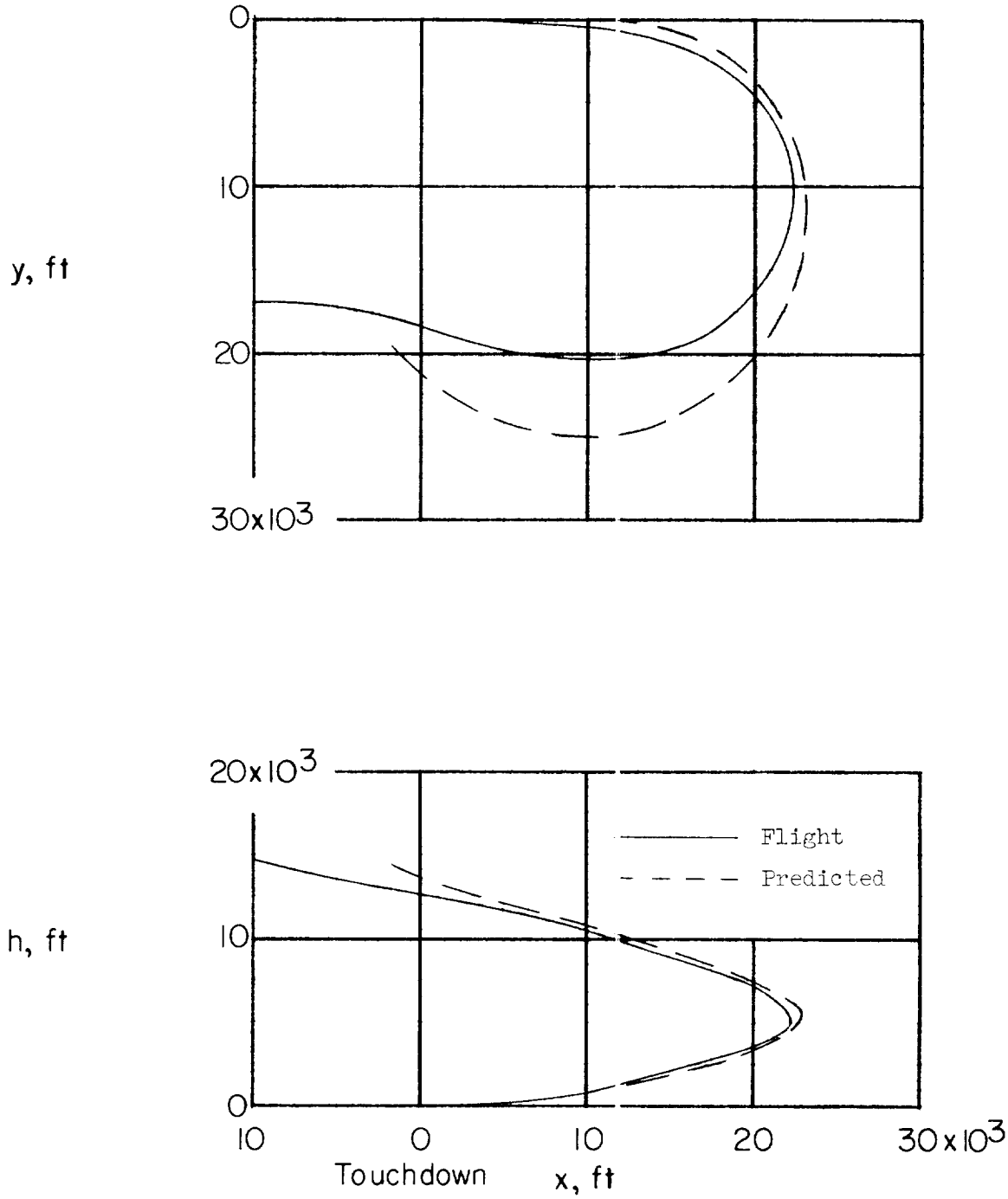

Figure 7.- Comparison of X-15 flight and predicted patterns.

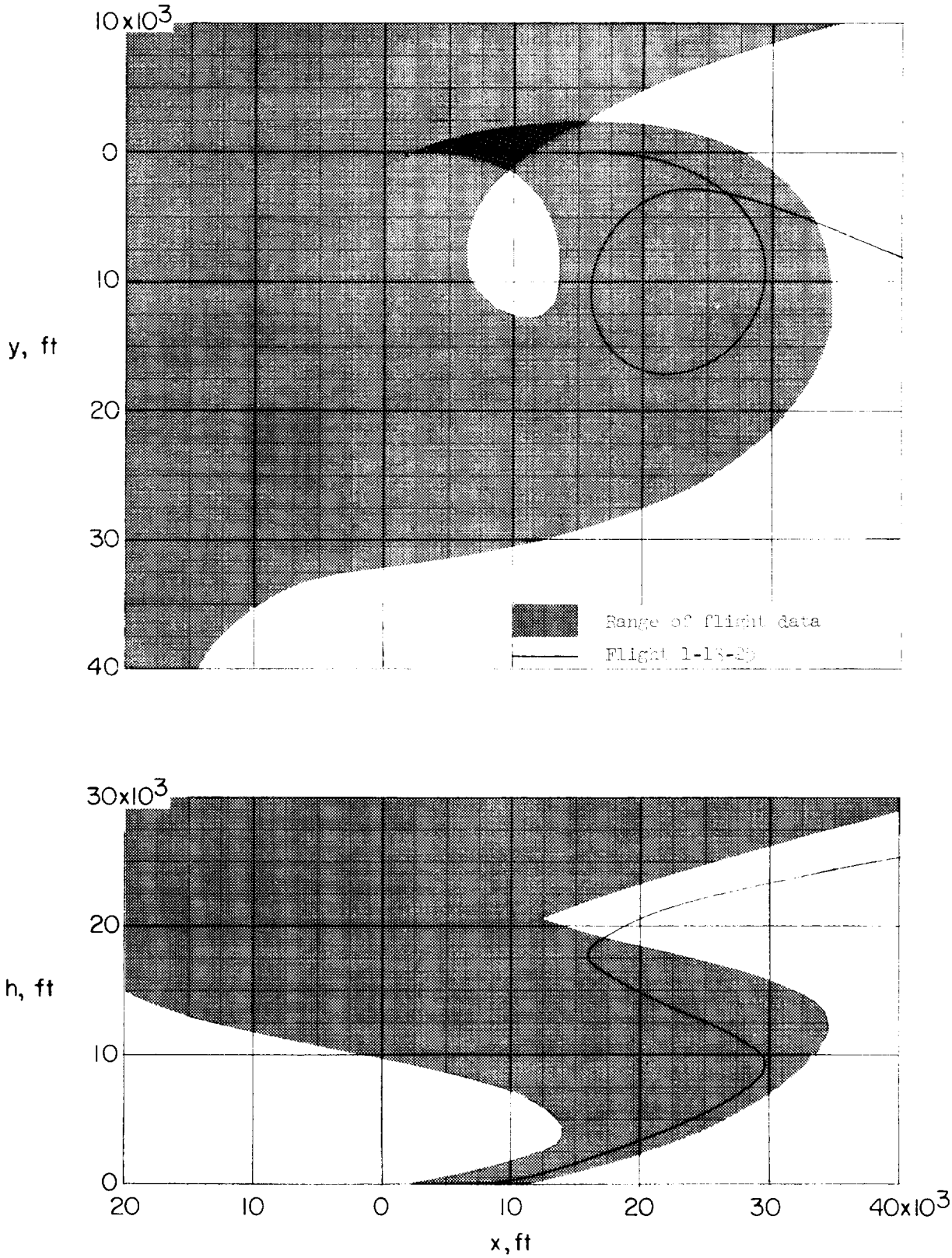

Figure 8.- Summary of X-15 landing patterns.

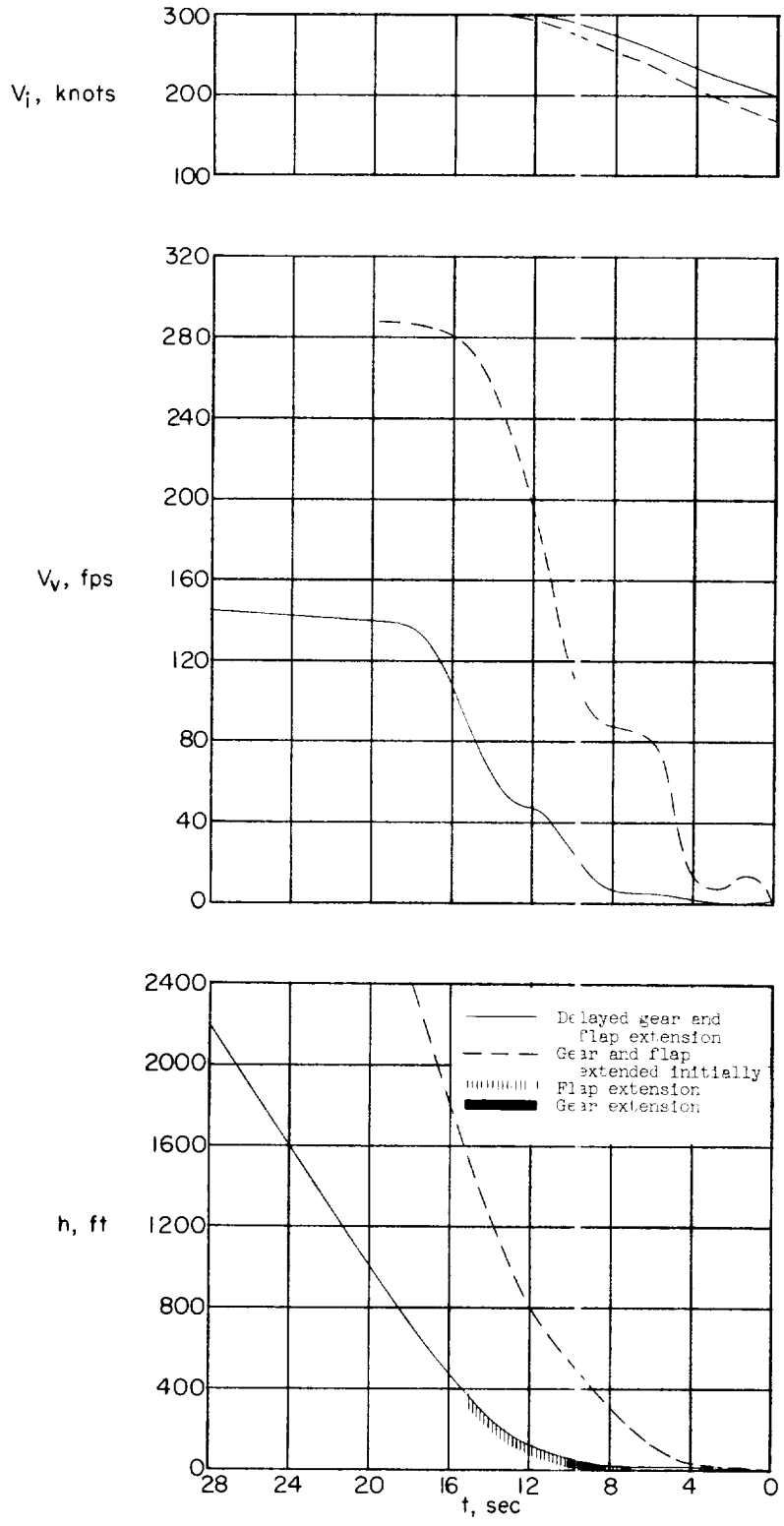

Figure 9.- X-15 analog simulation time history showing the effect of configuration on flare characteristics.

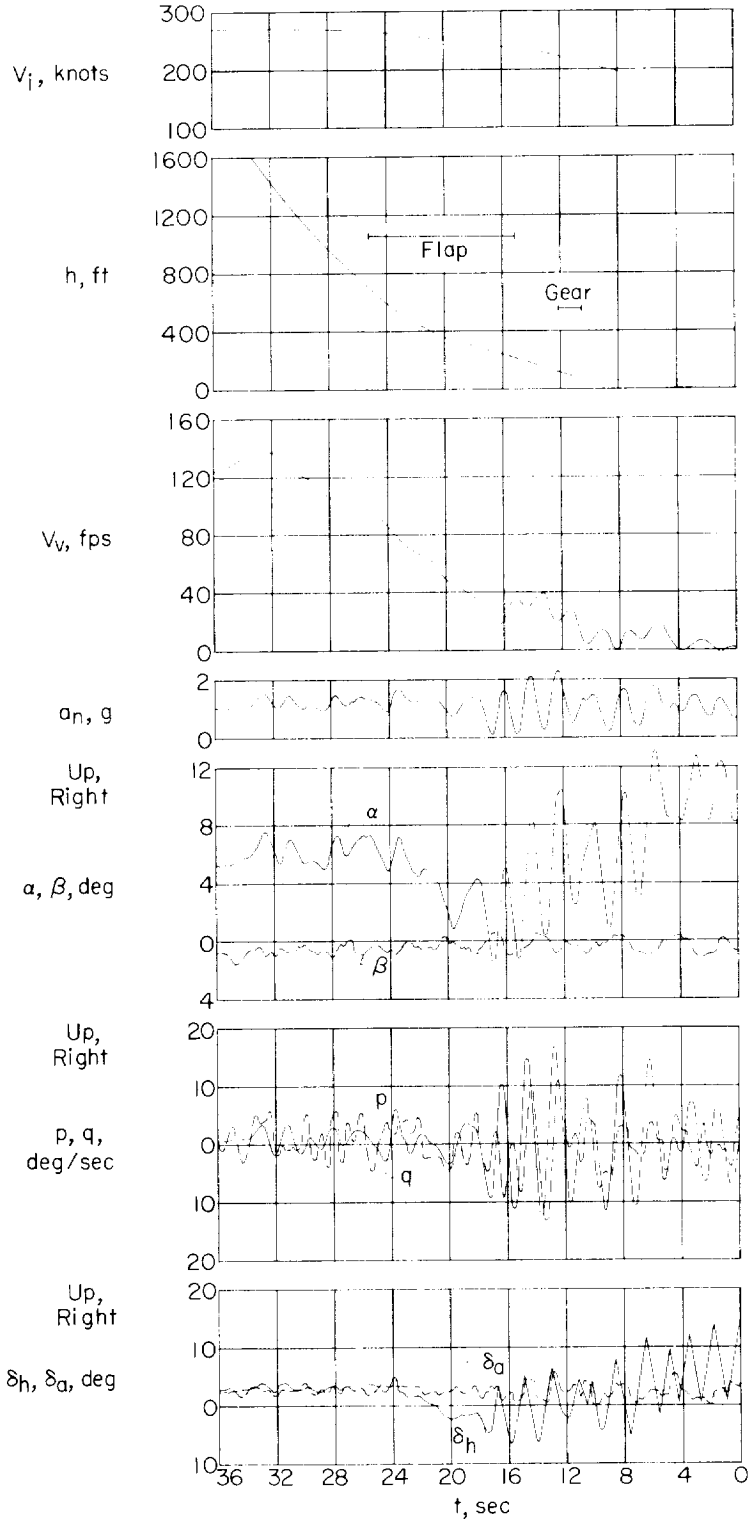

Figure 10.- Time history of the flare on X-15 flight 1-1-5.

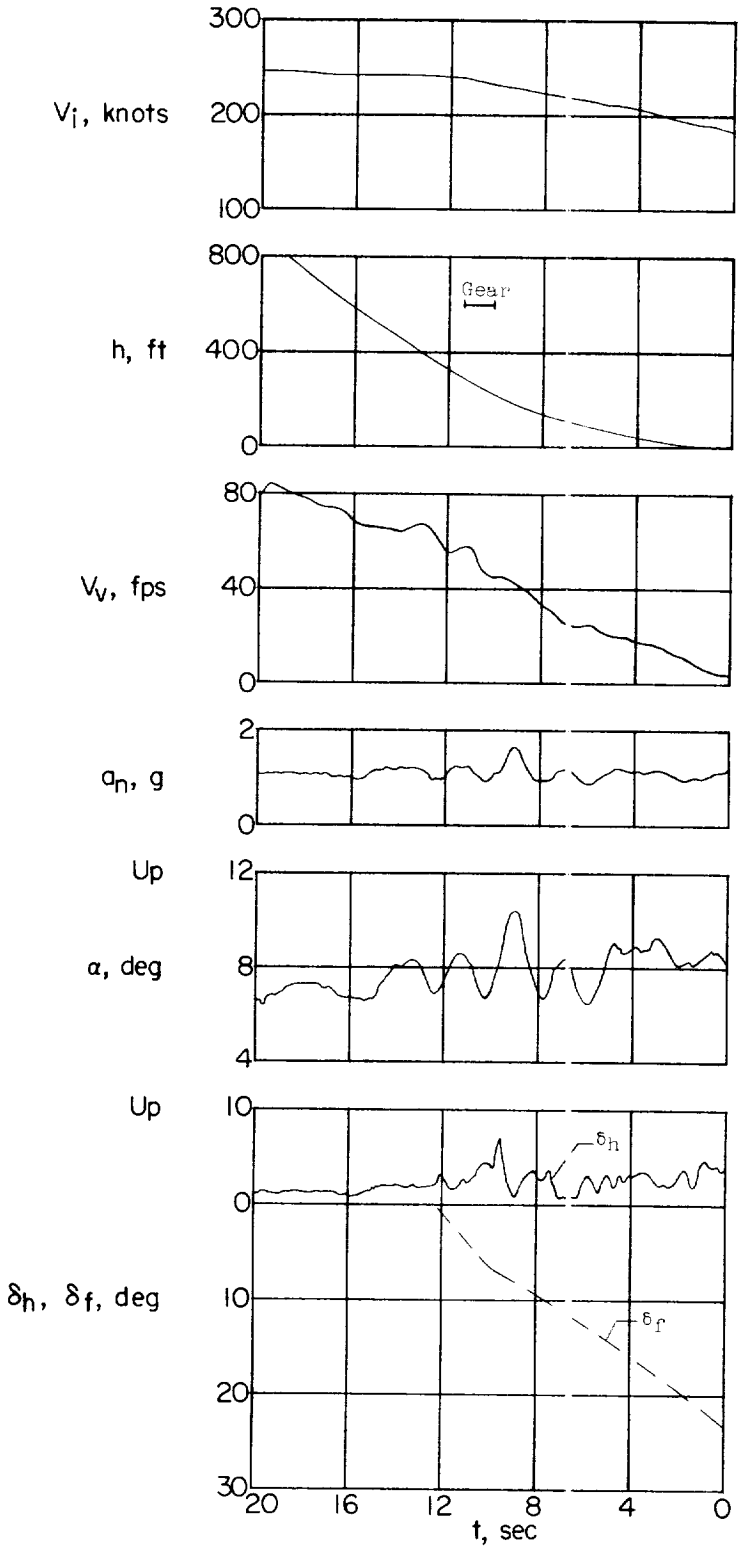

Figure 11.- Time history of the flare of X-15 flight 2-1-3.

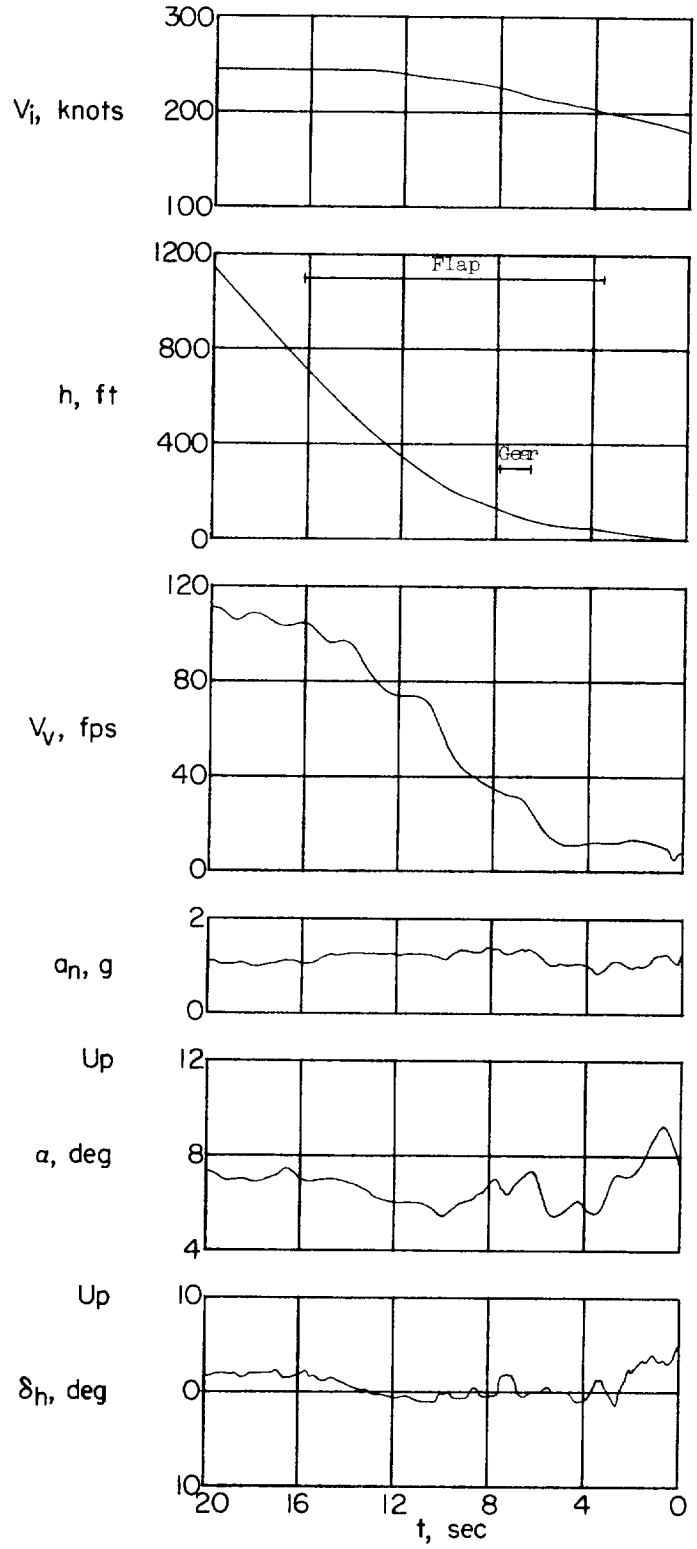

Figure 12.- Time history of the flare of X-15 flight 2-2-6.

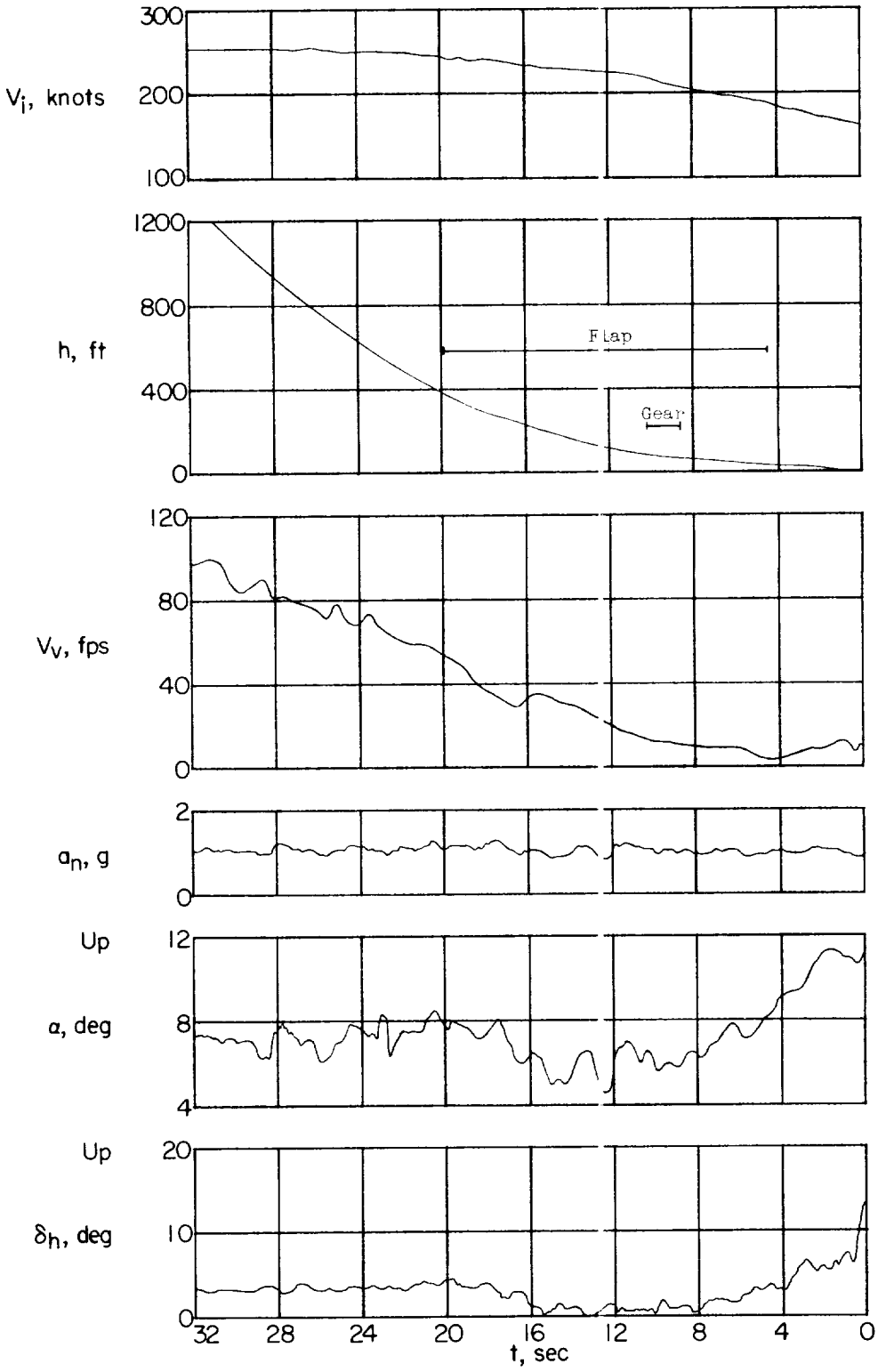

Figure 13.- Time history of the flare of X-15 flight 2-3-9.

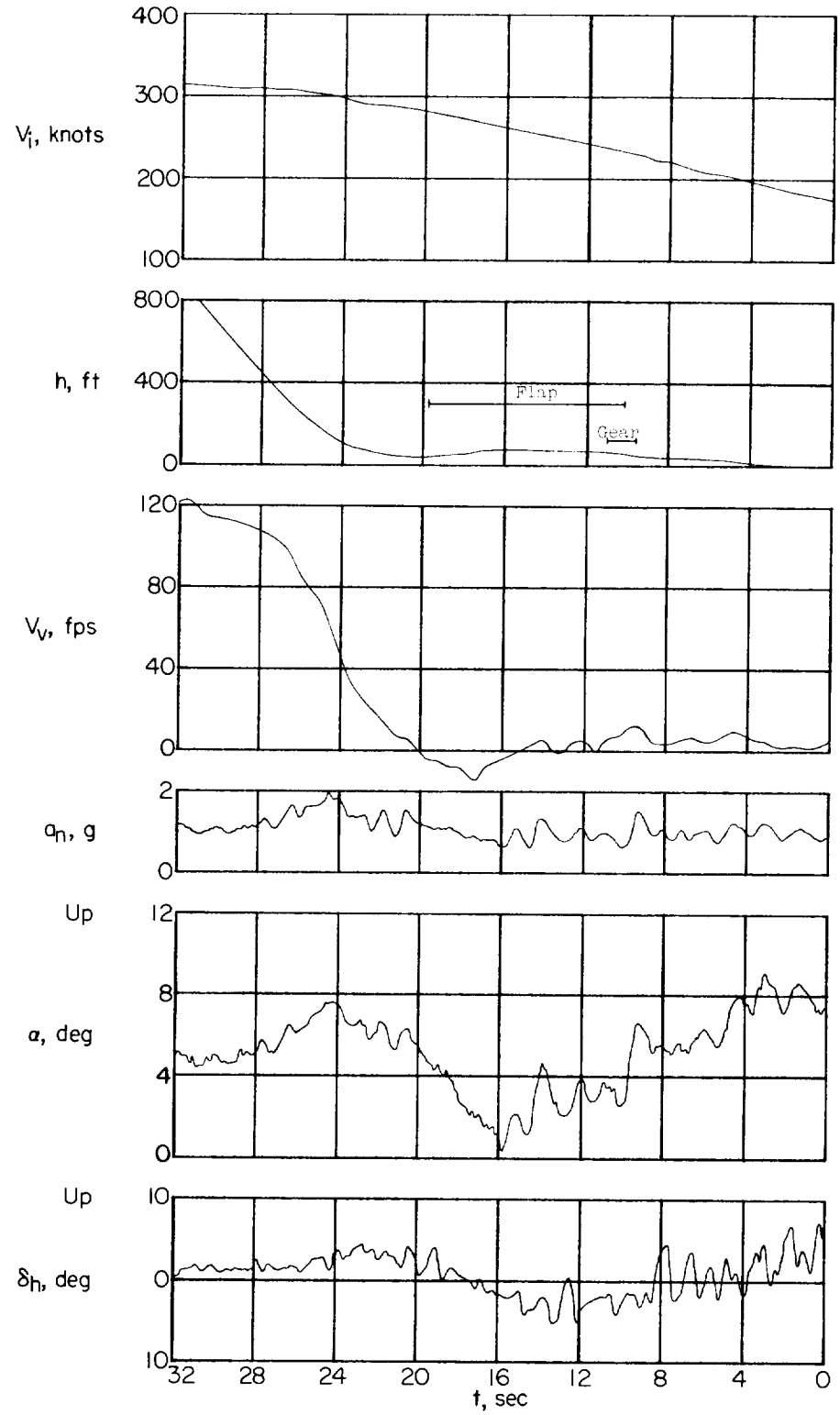

Figure 14.- Flare time history of X-15 landing with excess speed at flare initiation (flight 1-4-9).

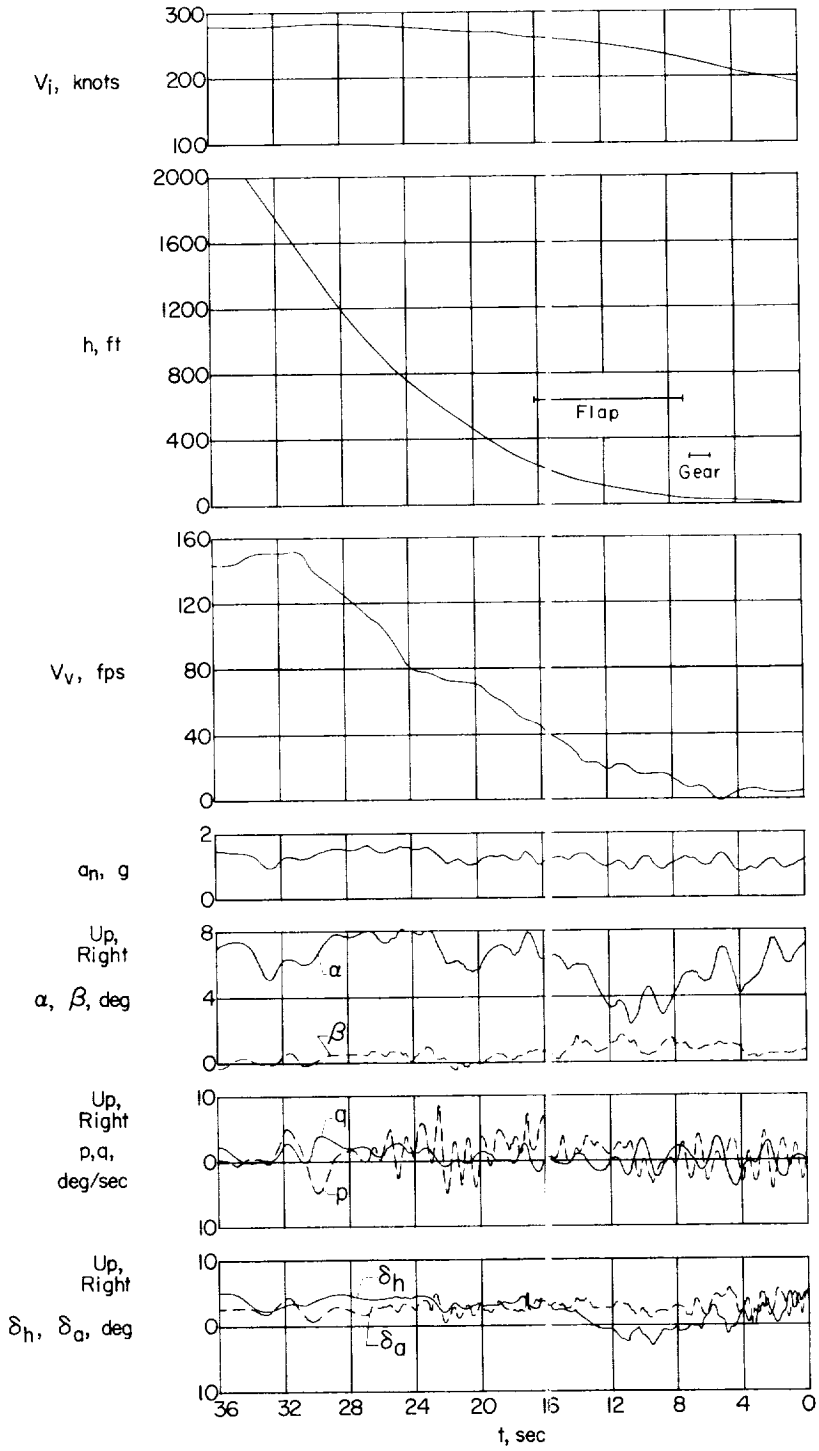

Figure 15.- Flare time history of X-15 with pitch damper inoperative (flight 1-2-7).

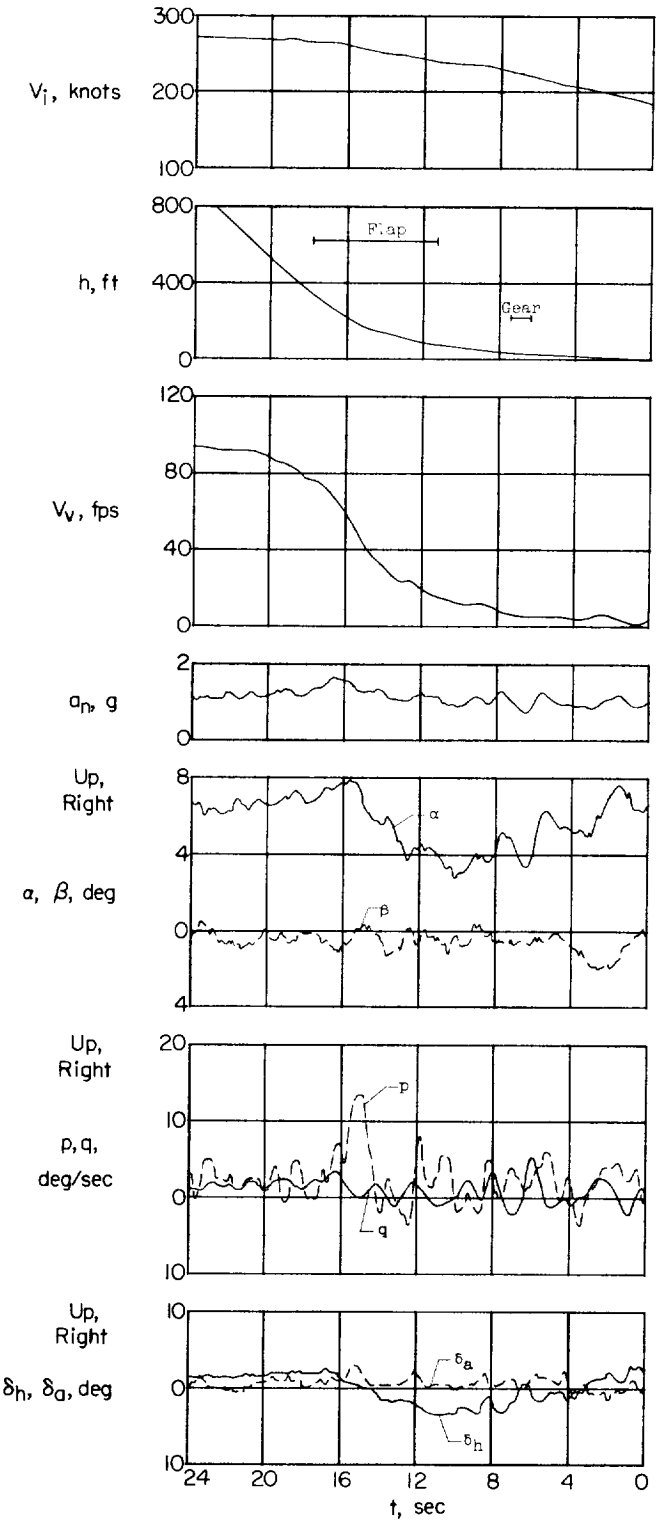

Figure 16.- Flare time history of X-15 landing with all dampers inoperative (flight 2-8-16).

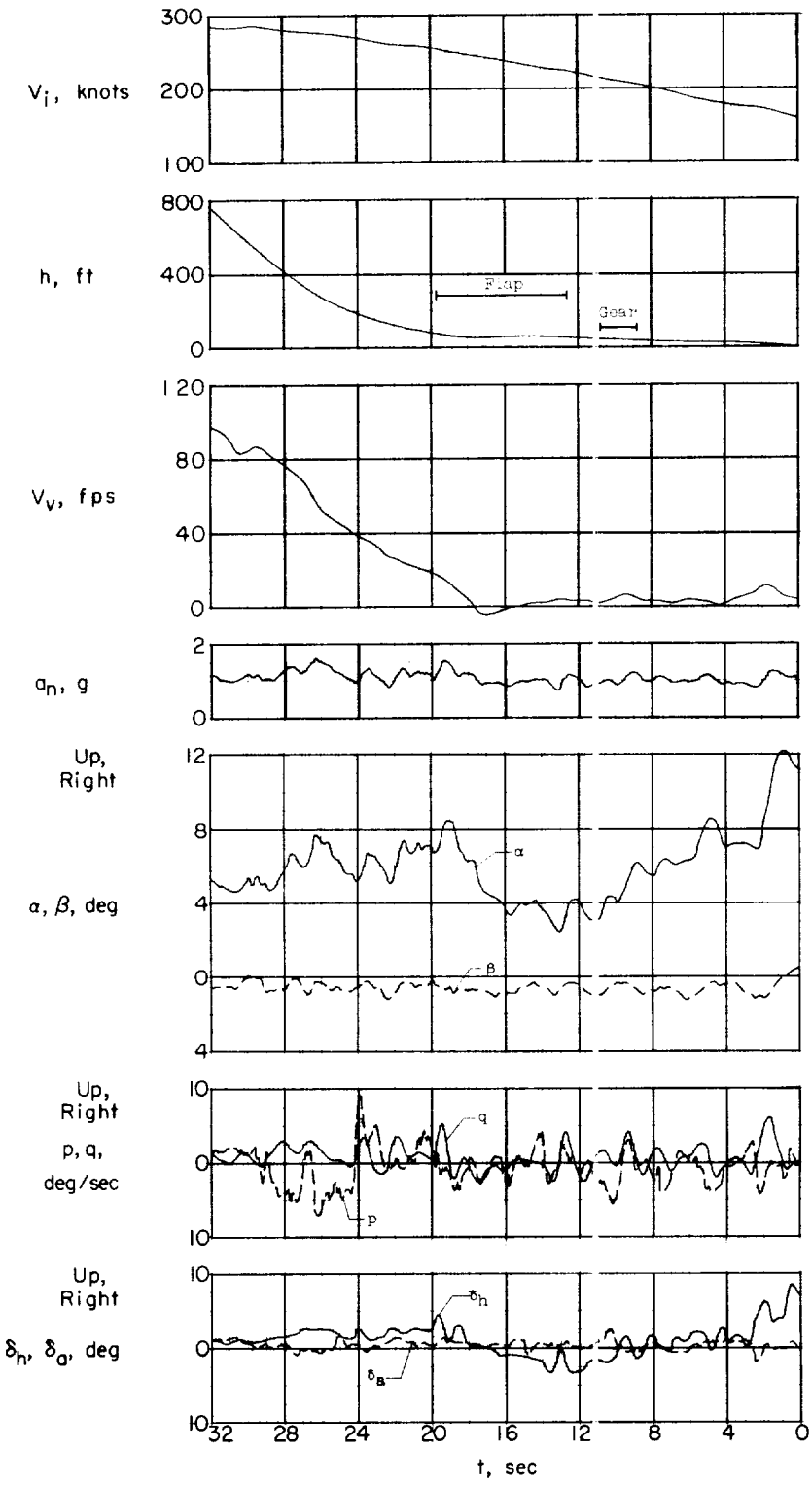

H-221

Figure 17.- Flare time history of X-15 larding using side-stick controller (flight 2-9-18).

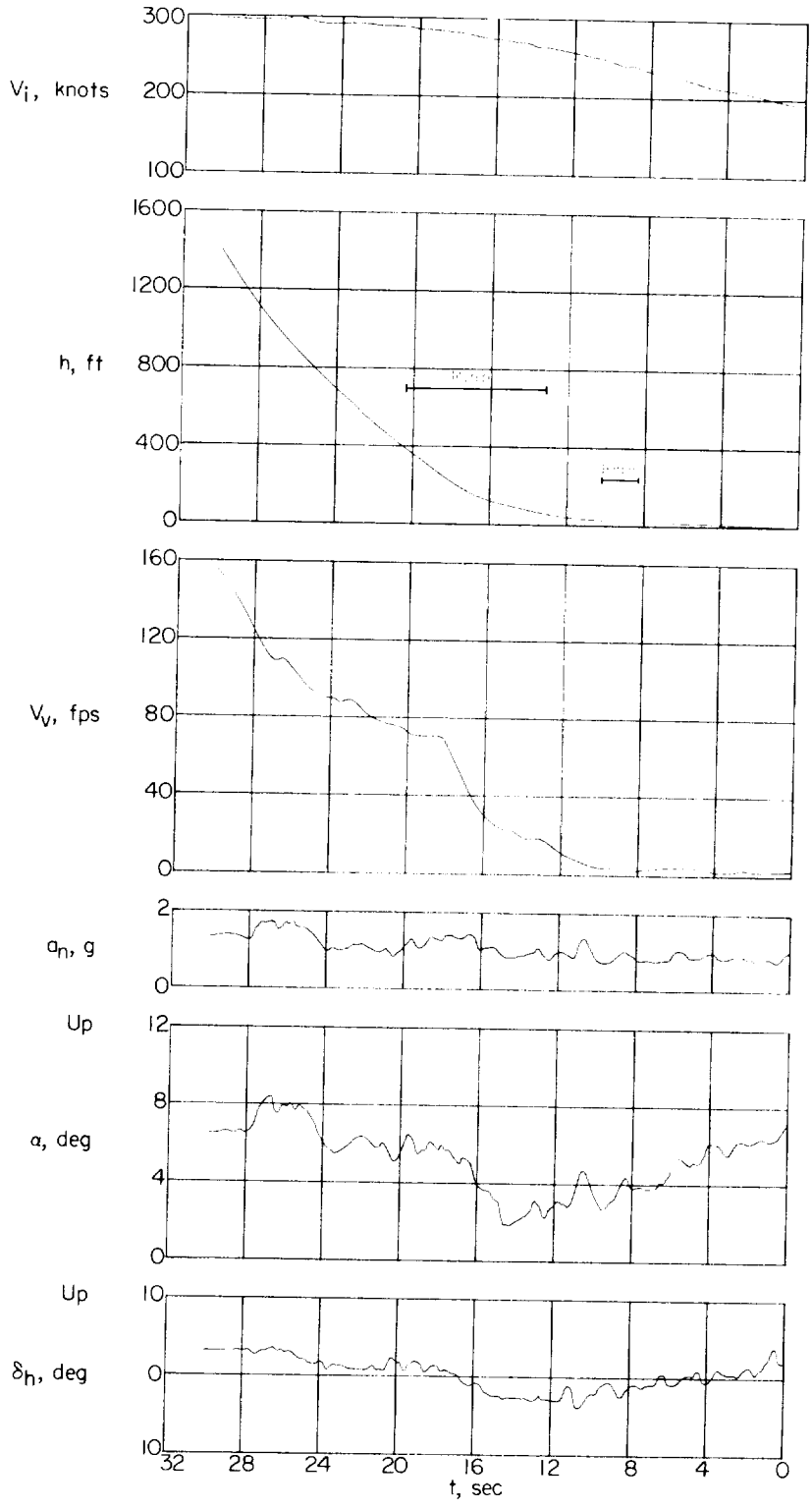

Figure 18.- Flare time history of X-15 landing with a flap deflection of 30° (flight 2-7-15).

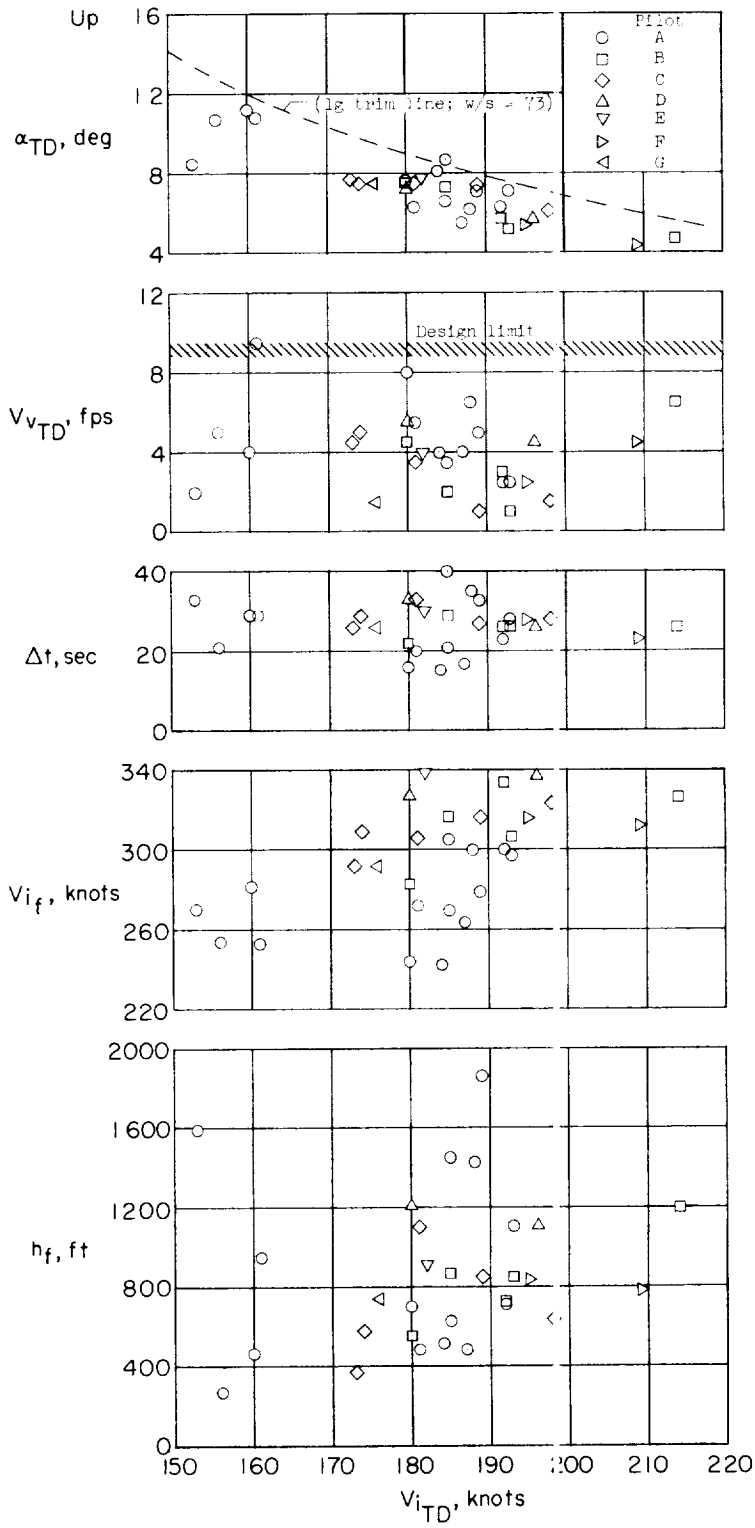

Figure 19.- Summary of X-15 flare and touchdown parameters.

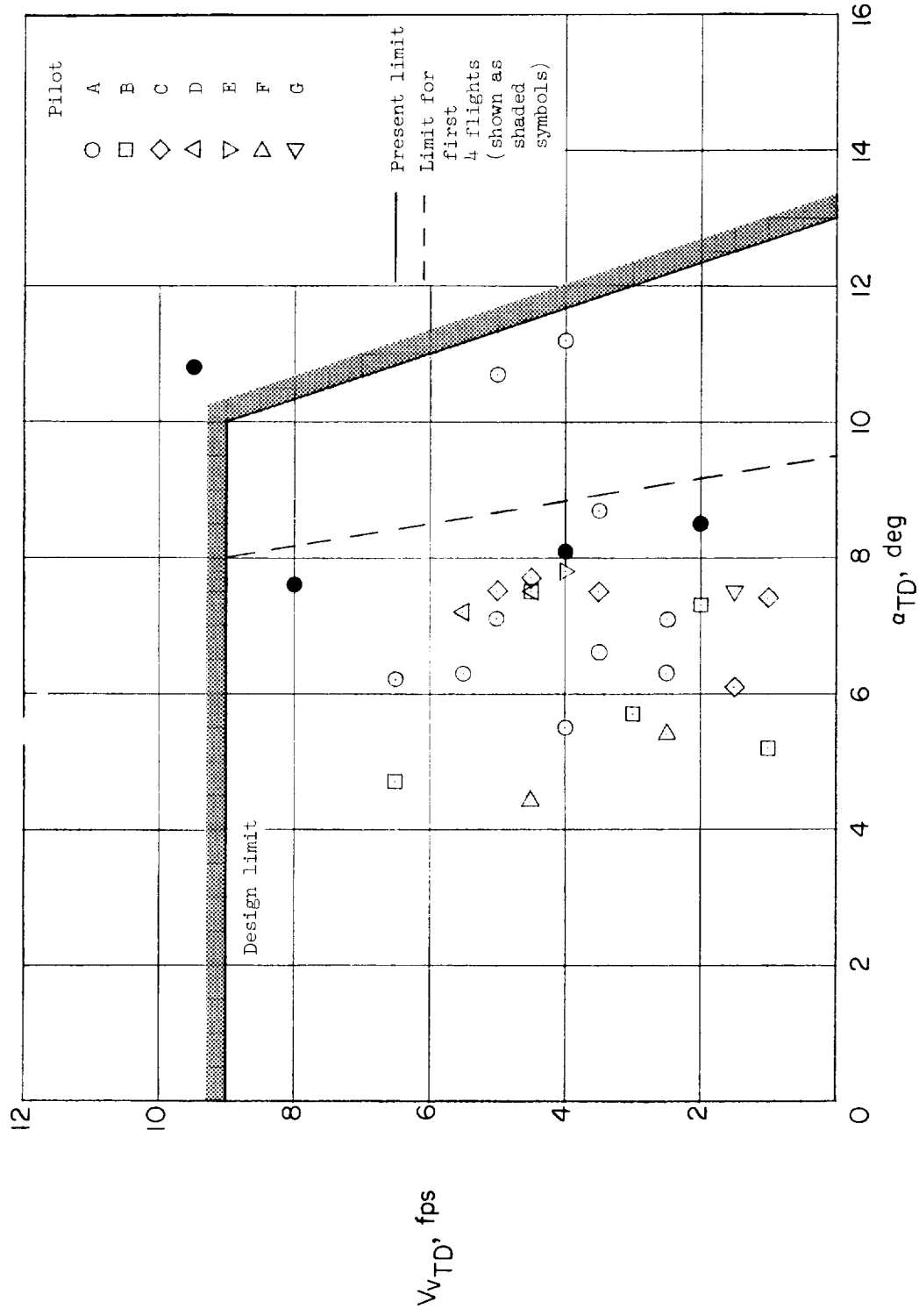

Figure 20.- X-15 gear design envelope in terms of touchdown angle of attack and vertical velocity.

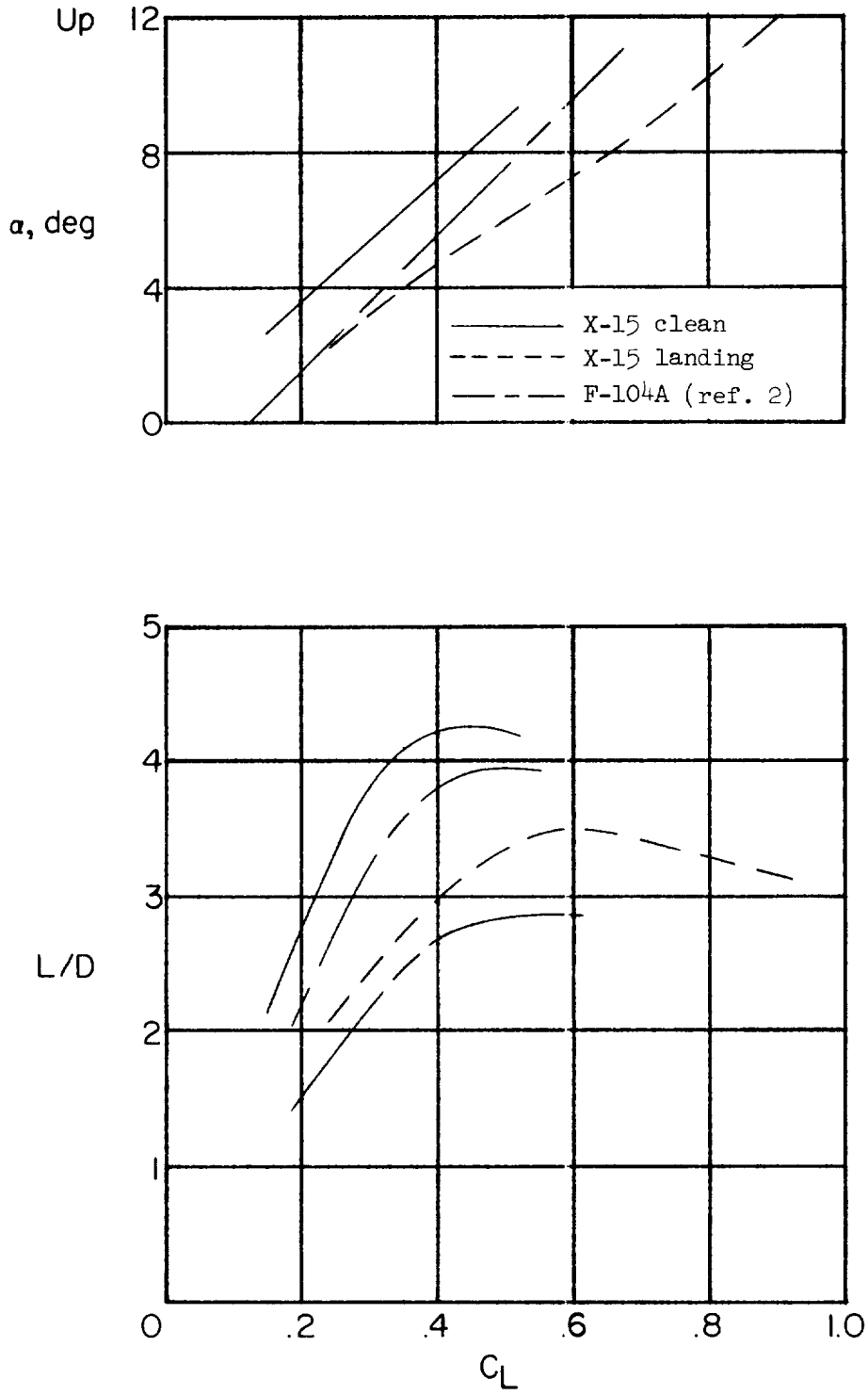

Figure 21.- Comparison of X-15 and F-104A performance data for approach and landing conditions.

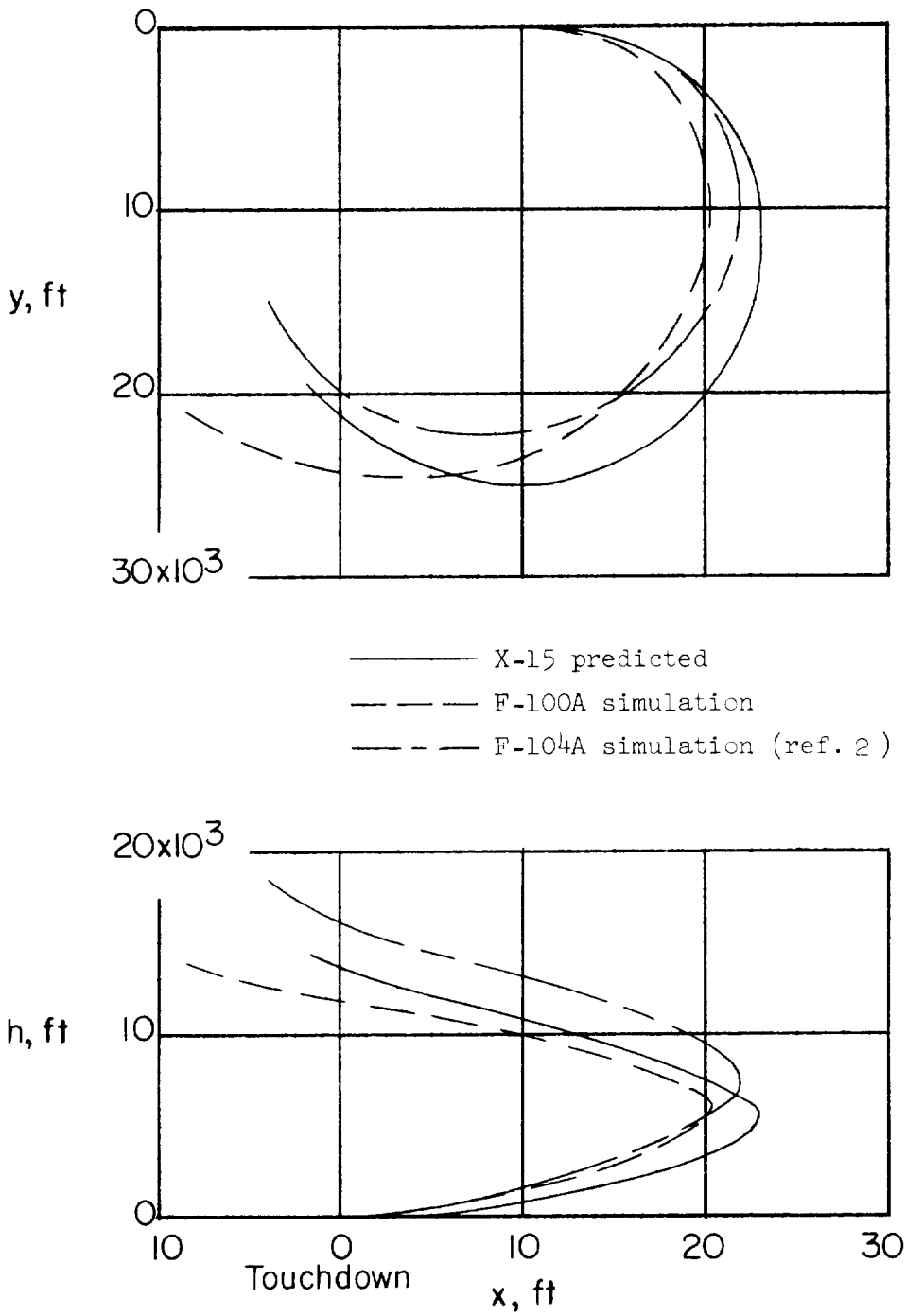

Figure 22.- Comparison of predicted X-15 pattern with flight-simulated patterns.

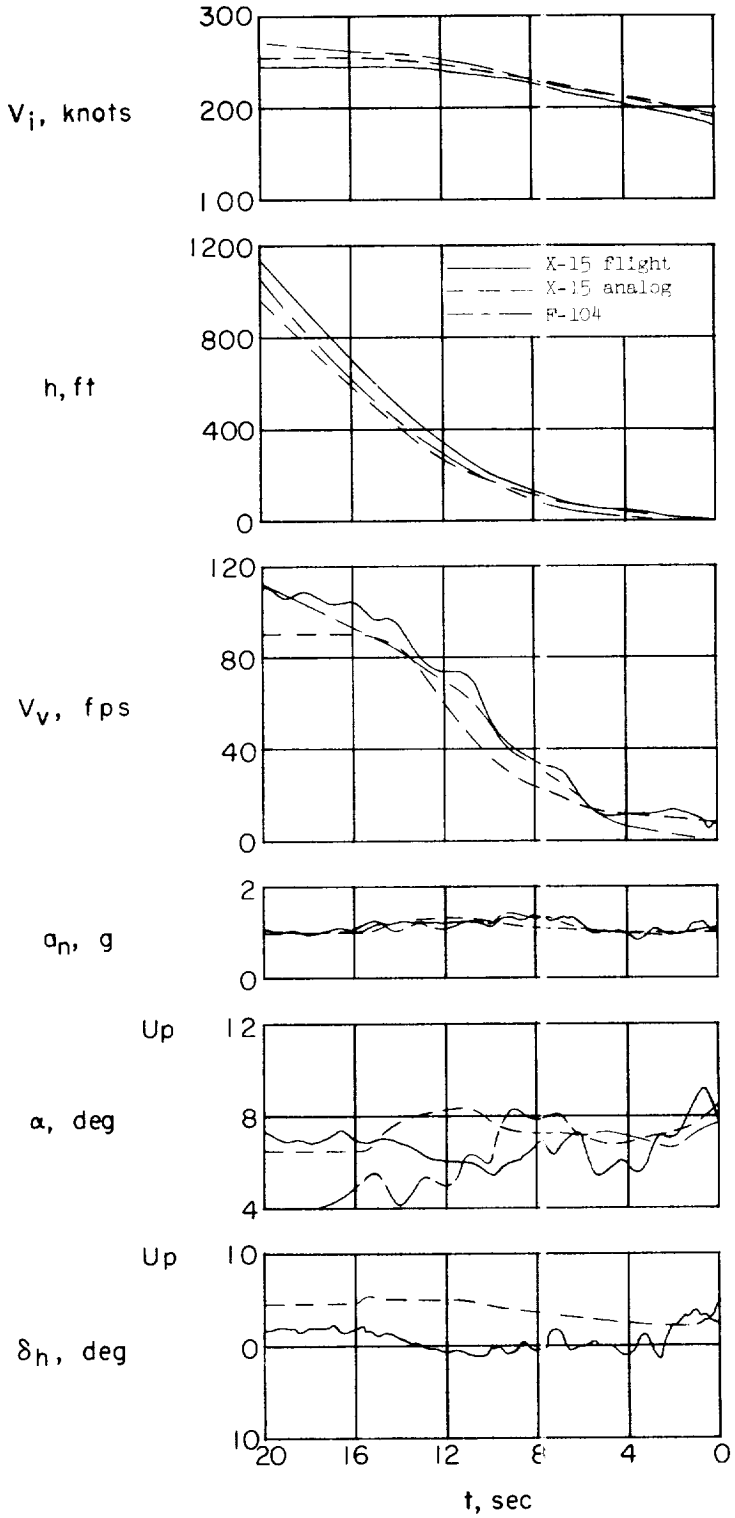

Figure 23.- Comparison of X-15 flight and simulated flares.

H-221